STUDY ON DRUG DELIVERY TARGETING OVARIAN CANCER CELLS March 2019 APRILIANA CAHYA KHAYRANI

STUDY ON DRUG DELIVERY TARGETING OVARIAN CANCER CELLS

March 2019

APRILIANA CAHYA KHAYRANI

Graduate School of Natural Science Technology

(Doctoral Course)

OKAYAMA UNIVERSITY

STUDY ON DRUG DELIVERY TARGETING OVARIAN CANCER CELLS

March 2019

APRILIANA CAHYA KHAYRANI

Graduate School of Natural Science Technology

(Doctoral Course)

OKAYAMA UNIVERSITY

Study on Drug Delivery Targeting Ovarian Cancer Cells

A dissertation submitted by **Apriliana Cahya Khayrani** in partial fulfilment of the requirements for the Doctor of Philosophy in Engineering in the Graduate School of Natural Science and Technology, Okayama University, Japan.

March 2019

Graduate School of
Natural Science and Technology
Okayama University

OKAYAMA UNIVERSITY
岡山大学

3.1.1 Tsushima-Naka
Kita-ku, Okayama 700-8530
Japan

February 25, 2019

CERTIFICATE

This is to certify that Mrs. Apriliana Cahya Khayrani has worked on the dissertation entitled "Study on Drug Delivery Targeting Ovarian Cancer Cells" under my supervision. This thesis is being submitted to the Graduate School of Natural Science and Technology, Okayama University for the partial fulfillment of the requirement for the degree of Doctor of Philosophy in Medical Bioengineering. It is an original record of the work conducted by the candidate and has not been submitted in full or part to any other university for the award of degree or diploma.

Masaharu Seno, PhD
Professor of Nano-Biotechnology,
Department of Medical
Bioengineering
Voice/Fax +81-86-251-8216
E-mail: mseno@okayama-u.ac.jp

CONTENTS

Say, "I am only a man like you, to whom has been revealed that your god is one God. So whoever would hope for the meeting with his Lord **let him do righteous work** and not associate in the worship of his Lord anyone." (Qur'an 18:110)

“Katakanlah: ‘Sesungguhnya aku ini hanya seorang manusia sepertimu, yang diwahyukan kepadaku: ‘Bahwa sesungguhnya Ilahmu itu adalah Ilah Yang Esa.’ Barangsiapa yang mengharapkan perjumpaan dengan Rabbnya, **maka hendaklah ia mengerjakan amal yang shalih** dan janganlah ia mempersekutukan seorang pun dalam beribadah kepada Rabbnya.” (QS. Al-Kahfi: 110)

قُلْ إِنَّمَآ أَنَا۠ بَشَرٌ مِّثْلُكُمْ يُوحَىٰٓ إِلَيَّ أَنَّمَآ إِلَٰهُكُمْ إِلَٰهٌ وَٰحِدٌ ۖ فَمَن كَانَ يَرْجُوا۟
لِقَآءَ رَبِّهِۦ فَلْيَعْمَلْ عَمَلًا صَٰلِحًا وَلَا يُشْرِكْ بِعِبَادَةِ رَبِّهِۦٓ أَحَدًۢا ﴿١١٠﴾

Summary

Ovarian cancer is the most lethal gynecologic malignancy, it ranks the eighth cause of cancer death in women of worldwide. The standard treatment of progressive ovarian cancer is surgical resections followed by systemic chemotherapy. The National Comprehensive Cancer Network (NCCN) guideline shows as first line chemotherapeutic agents for ovarian cancer the carboplatin, paclitaxel (PTX) or the administration in combination of these two

PTX acts as an anti-cancer agent preventing cells division by promoting and stabilizing the assembly of microtubule structures. Because PTX is highly hydrophobic the mixture of Cremophor EL® and ethanol has been adopted as solvent for the commercial formulation known as Taxol. Nonetheless, administration of Taxol may cause side effects such as hypersensitivity reactions, nephrotoxicity and neurotoxicity. Therefore, the disadvantages of Taxol treatment should urgently be ameliorated by the development of proper drug delivery system of PTX. The highly hydrophobic nature of PTX hinders the loading efficiency into the liposomes resulting in a poor encapsulation yield. Recently, we successfully developed liposomes encapsulating glycosylated paclitaxel (gPTX) in the hydrophilic core. gPTX is a PTX derivative with a glucose moiety coupled at the 7-OH radical. This modification enhanced the hydrophilicity of PTX allowing its solubility in different solvents CEP (Cremophor EL®, ethanol, and PBS; in 12:12:76 ratio) and EG (40% Ethylene Glycol). Exploiting the difference of the solubility we could prepare stable gPTX liposome (gPTX-L) with sufficient amount of encapsulated drug.

The outer layer of liposomes can be modified with coupled ligands targeting molecules localized on the cell membrane surface. Targeted-drug delivery nanosystems with coupled ligands have been actively utilized to optimize therapeutic

efficacy and minimize systemic toxicity. Ligands for cell surface receptors highly expressed in tumor cell populations have provided a great specificity. The cell membrane receptor CD44 could be one of the most promising candidates to be targeted. CD44 is a receptor for hyaluronic acid type-1 transmembrane glycoprotein that is implicated in cell–cell and cell–matrix interactions and is associated with malignancy, particularly with metastasis promotion. CD44 has also been considered as a cancer stem cell (CSC) marker in several malignancies of hematopoietic and epithelial origin, and is closely related with tumor progression and drug resistance in several tumors including ovarian cancer. Collectively, CD44 could be a suitable candidate molecule to be targeted by the drug delivery nanosystem as ovarian cancer therapeutic.

In this study, we have optimized the loading efficiency of gPTX achieving higher encapsulation yields of gPTX-L, and have also designed the immunoliposome CD44-targeted gPTX-IL. To generate gPTX-IL, the anti-human CD44 monoclonal antibody (anti-hCD44 MAb) was conjugated to the gPTX-L and its efficacy was evaluated under *in vitro* and *in vivo* conditions.

CHAPTER 1

General Introduction

Ovarian Cancers

Ovarian cancer causes more deaths in the United States than any other type of female reproductive tract cancer, with an estimated 22.240 new cases and 14.070 deaths in 2018 [1]. Ovarian cancer accounts for just 2.5% of all female cancer cases, but 5% of cancer deaths because of the disease's low survival. This is largely because 4 out of 5 ovarian cancer patients are diagnosed with advanced disease that has spread throughout the abdominal cavity. Overall ovarian cancer incidence rates have been decreasing since the mid-1980s, with the pace of the decline accelerating in the early 2000s[1,2].

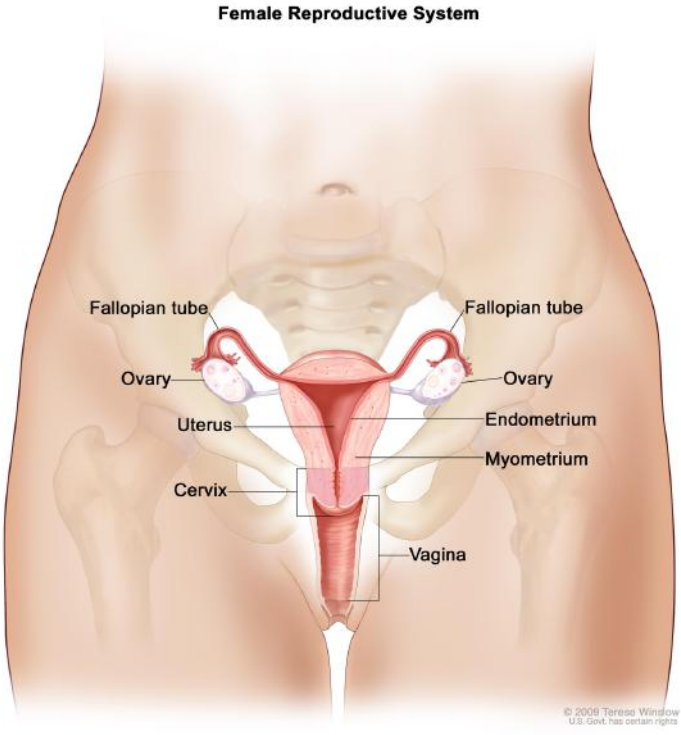

Figure 1. Normal female reproductive anatomy. (originally published by the National Cancer Institute)

The ovaries are a pair of reproductive glands, each about the size of a grape, located on either side of the uterus (Figure 1). They produce eggs that travel through the

fallopian tubes into the uterus, where they are fertilized for reproduction. In premenopausal women, the ovaries are the primary source of the hormones estrogen and progesterone, which maintain the health of the female reproductive system. The three major types of ovarian cancer are epithelial, accounting for 90% of cases, germ cell (3%), and sex cord-stromal (2%). Epithelial cancers are further subdivided into serous (52%), endometrioid (10%), mucinous (6%), and clear cell (6%) tumors[3,4].

Ovarian cancer is not easily diagnosed because the most common presenting symptoms of persistent abdominal distension — pain and pressure in the pelvis — can be attributed to a number of causes[5]. Patients may be asymptomatic until an abdominal mass is discovered during routine pelvic examination or until the tumour has metastasised [6], consequently, progression to late stage before diagnosis is seen in the majority of presenting women. Approximately 75% of patients are at International Federation of Gynecology and Obstetrics (FIGO) stages II–IV at the time of diagnosis [5].

Ovarian Cancer Treatment

Surgery is currently the intervention of first choice in ovarian cancer [5]. In advanced cases, tumour debulking is recommended to improve the efficacy of adjunctive therapies. Optimal debulking can be achieved in the majority of patients, and prognosis is directly related to the success of such cytoreductive surgery [6].

Chemotherapy for ovarian cancer has progressed considerably over the past two decades, with treatment for advanced disease moving from the use of alkylating agents to current recommended regimens based on taxanes and platinum compounds [5,6].

Clinical trials performed in the late 1970s demonstrated that cisplatin was an active chemotherapy in advanced or recurrent ovarian cancer with a single agent response rate in the range of 13–30% [7,8]. The next generation of research studies evaluating

combination chemotherapy with cisplatin plus cyclophosphamide revealed that the time to progression and the duration of survival were markedly improved compared with single agents [9]. As the result, the standard combination chemotherapy in the late 1980s and early 1990s was cisplatin plus cyclophosphamide. Carboplatin was introduced in the 1990s as an analog of cisplatin with similar single-agent activity in terms of response and survival rates, but with a significantly improved toxicity profile. Paclitaxel, an active chemotherapeutic agent introduced in the 1990s, changed the standard of care in ovarian cancer yet again. Two randomized clinical trials comparing cyclophosphamide and cisplatin with paclitaxel and cisplatin demonstrated that the investigational arm had an improved outcome compared with the previous standard combination of cyclophosphamide and cisplatin [10,11].

From the past 20 years, the standard of care in advanced ovarian cancer for ovarian cancer encompasses administration of platinum, paclitaxel, or the combination of platinum plus paclitaxel.

Paclitaxel (PTX)

Between 1960 and 1981, the National Cancer Institute (NCI) and the U.S. Department of Agriculture (USDA) collaborated on a plant screening program that collected and tested 115,000 extracts from 15,000 species of plants to identify naturally occurring compounds with anticancer activity. In 1963, a crude extract from the bark of the Pacific yew Taxus brevifolia, a scarce and slow-growing evergreen found in the old-growth forests of the Pacific Northwest, was found in preclinical studies to have cytotoxic activity against many tumors [12]. PTX was identified as the active constituent of this extract in 1971 by Mansukh Wani and Monroe Wall. They had isolated and identified the active ingredient and named it taxol (generic name of

PTX), based on its species of origin and the presence of hydroxyl groups [13] and it entered the NCI drug development program.

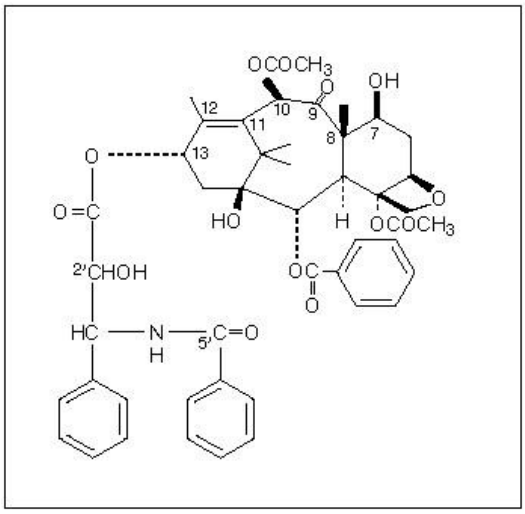

Figure 2. Structure of PTX (Rowinsky EK, Donehower RC. N Engl J Med 1995;332:1004-1014)

In 1979, Susan Horwitz at Albert Einstein College of Medicine (New York, NY), reported that PTX promotes the assembly of microtubules—polymers composed of repeating subunits of α- and β-tubulin heterodimers. PTX reduces the critical concentration of purified tubulin subunits necessary for polymerization into microtubules *in vitro* and increases the percentage of tubulin subunits that assemble. Furthermore, microtubules polymerized in the presence of PTX are protected from the disassembly normally induced by cold or calcium treatment [14]. These effects were in stark contrast to previously identified microtubule poisons, including colchicine and vinca alkaloids, which prevent microtubule polymerization [15]. Similar to its effects on purified tubulin, PTX promotes microtubule polymerization and stabilization in living cells, where it is capable of antagonizing the effects of colchicine and vinca alkaloids [14].

PTX-induced mitotic arrest occurs due to activation of the mitotic checkpoint (also known as the spindle assembly checkpoint), the major cell cycle control mechanism acting during mitosis to prevent chromosome missegregation. The mitotic checkpoint delays separation of the chromosomes, which enter mitosis as replicated pairs of sister chromatids, until each pair has made stable attachments to both poles of the mitotic spindle. This arrangement ensures that each daughter cell will receive one copy of every chromatid. Chromatids connect to spindle microtubules through their kinetochores, protein complexes that assemble on centromeric regions of DNA. Unattached kinetochores, which have not made stable attachments to microtubules, activate a signal transduction cascade that delays mitotic progression by inhibiting the anaphase-promoting complex/cyclosome [16]. PTX treatment arrests cells in mitosis due to the presence of a small number of unattached kinetochores [17].

In spite of its promising anticancer activity, the development of intravenous PTXs formulation has showed several difficulties due to its poor solubility in water. According to this, the first commercially available formulation containing PTX (Taxol®) is formulated in a vehicle composed of polyoxyethylated castor oil (Cremophor® EL) and dehydrated alcohol in equal parts. Thus, the current clinical dosage form contains in each millilitre 6 mg of PTX, 527 mg of Cremophor® EL (CrEL) and 49.7% (v/v) of absolute ethanol. This vehicle is associated with a variety of side effects such as hypersensitivity, nephrotoxicity and neurotoxicity, attributable mainly to Cremophor® EL. Importantly, these effects are shown in 25–30% of treated patients [18]. Thus, the amount of CrEL administered (for an average patient for a single dose administration) with these drugs averages 5 mL, whereas the amount of CrEL in Taxol® per administration is the relatively higher, approximately 26 mL [19]. Consequently, all patients receiving Taxol® must be premedicated with corticoids, H_2 antagonists and antihistamines to prevent, sometimes fatal, hypersensitivity reactions.

Moreover, CrEL has a direct influence over the cells of the pulmonary and vascular endothelium, causing respiratory difficulties and vasodilatation. Severe reactions as bronchospasms and hypotension have been reported [20]. Furthermore, since both ethanol and CrEL solubilize the plasticizers, Taxol® requires the use of non-plasticized solution containers such as di(2-ethyl-hexyl) pthalate (DEHP) in the polyvinylchloride (PVC) infusion bags/sets (Rowe et al., 2009).

Since CrEL can cause hypotension and hypersensitive reactions, Taxol® should be slowly infused over a period of 3 to 24 h for doses of 135–175 mg/m2 every 3 weeks, respectively [21]. It should be previously diluted at a final concentration of 0.3 to 1.2 mg/mL, thus depending on the dose volumes ranging from 250 to 1000 mL of physiological solution or dextrose 5% may be required. Also, due the risk of drug precipitation upon dilution, Taxol® should be administered using an in-line filter (≤0.22 μm). A considerable number of clinic studies with Taxol® have been performed to date and have revealed highly variable pharmacokinetics [22]. The half-life was found to be in the range of 1.3 and 8.6 h and a large volume of distribution of about 55 L/m2 was also reported [23]. PTX is more than 90% bound to plasma proteins. The main pathways of elimination are hepatic metabolism followed by biliary excretion. In the liver, metabolism is mediated by the cytochrome P450 (CYP3A4 and CYP2C8) and less than 10% of the dose is excreted intact by urine [24]. This drug has shown a variable pharmacokinetic pattern depending on the infusion time. Early studies for prolonged infusion times (6 or 24 h) were generally suggestive of linear pharmacokinetics, but become nonlinear for shorter durations infusion (3 h) due to saturable elimination [25]. The clinical relevance of nonlinear deposition of the drug is based on the fact that small changes either in dosage or infusion duration might result in systemic exposure levels of PTX too large, thereby increasing the risk of toxicity. For example, 3-h infusions of PTX at 135 mg/m2 resulted in a mean Cmax

of 3.3 mM and a mean AUC of 10.4 μMh, whereas at 175 mg/m2, the mean Cmax and AUC values were 5.9 and 18.0 μMh, respectively [26]. Moreover, various studies have shown that CrEL alters the pharmacokinetics profile of the drug and contribute to the reduction in plasma clearance observed at higher PTX doses. Indeed, PTX may be entrapped within hydrophobic interior of CrEL micelles in plasma, which tend to diminish the free fraction of PTX and, thus making it less available for distribution to tumor [27].

Generally, the main reason for discontinuation of PTX is not the lack of efficacy, but toxicity [28]. Peripheral sensory neuropathy is the most commonly reported neurotoxic effect of PTX which is dose- and infusion-duration related [29]. The symptoms may begin as early as 24–72 h after administration and include numbness, paresthesias and burning pain in a glove and-stocking distribution. Because CrEL can also cause neurotoxicity, PTX-induced neuropathy may be at least, in part, contributed by the vehicle formulation [19]. The other major adverse effect is myelosuppression, which mainly consists of neutropenia and usually becomes the dose-limiting toxicity [30].

Glycosylated Paclitaxel (gPTX)

Side effects of PTX in the cancer treatment due to its highly hydrophobicity resulted in massif research on the development or modification of PTX, including our laboratory. We developed glycosylated PTX (gPTX), a PTX derivative with a glucose moiety coupled at the 7-OH, this modification enhanced the hydrophilicity of PTX allowing practically different solubility in the solvents CEP (Cremophor EL®, ethanol, and PBS; in 12:12:76 ratio) and EG (40% Ethylene Glycol)[31].

The preparation of gPTX is occupied commercially available PTX. It was treated with TESCl and N, N- diisopropylethylamine as a base in methylene chloride,

providing 20- triethylsilyloxyPTX (20-TES-PTX) at 97% yield, which was reacted with protected glucosyloxyacetic acid [32,33] using EDCI/DMAP/CH2Cl2 to furnish an inseparable mixture of 20- TES-7-a-gPTX and 20-TES-7-b-gPTX (20-TES-7-gPTX) at 78% combined yield. Triethylsilyl, trityl and benzyl groups were cleanly removed in a single step through a catalytic hydrogenation as described earlier, providing gPTX at 83% yield (Figure 3A). The 20-TES-7-gPTX was condensed with protected a-glucosyloxyacetic acid or protected b-glucosyloxyacetic acid [33] using EDCI/DMAP/CH2Cl2 to give 20-TES-7-a-gPTX at 78% yield or 20-TES-7-b-gPTX at 76% yield. Deprotection of triethylsilyl, trityl, and benzyl groups was accomplished in the same manner as described earlier providing 7-a-gPTX at 83% yield and 7-b-gPTX at 80% yield, respectively (Figure 3B and C)

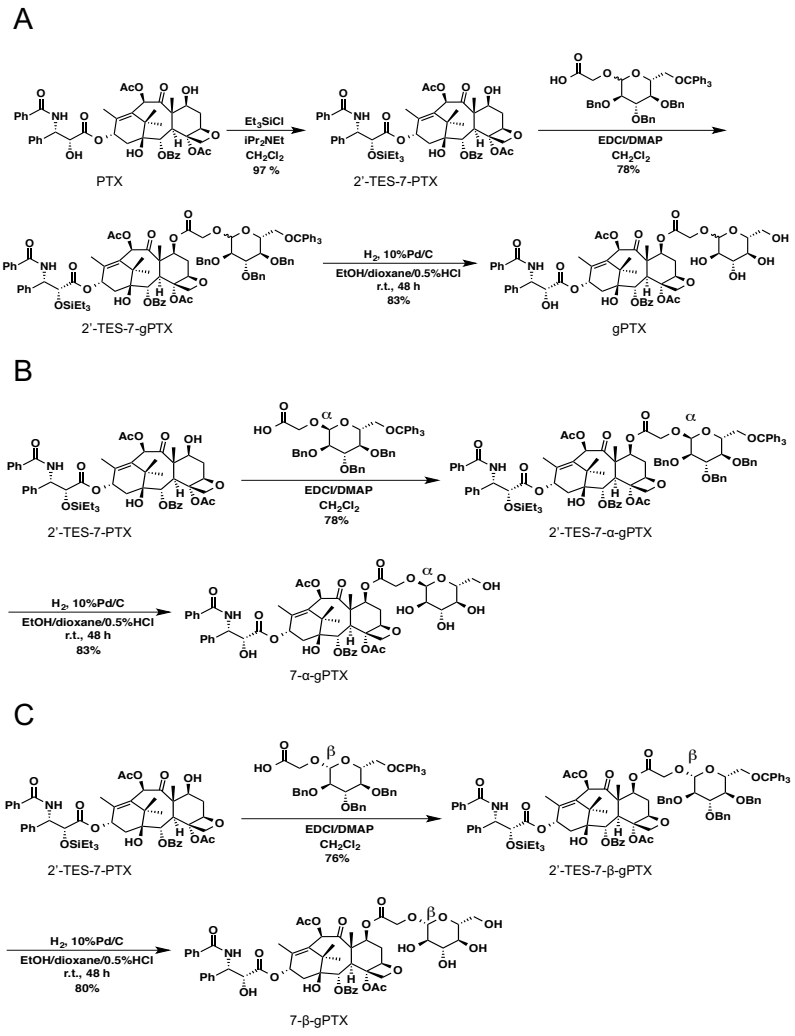

Figure 3. Synthesis of 7-glucosyloxyacetylPTXs (gPTX). (A) scheme of gPTX as a mixture of 7-α-gPTX and 7-β-gPTX. (B) scheme of 7-α-gPTX. (C) scheme of 7-β-gPTX (Shigehiro,T, et al, Journal of Microencapsulation, 2016, 33:2, 172-182).

Liposomes Based Drug Delivery System

Drug delivery is the method or process of administering a pharmaceutical compound to achieve a therapeutic effect in humans or animals. Recently, nanotechnology and nanoscience based drug delivery present a highly positive prospective of bringing benefits to many research areas and applications. Nanosized vehicles have received considerable attention over the past 30 years as pharmaceutical carriers with a wide range of applications, including drug delivery vehicles, adjuvants in vaccinations, signal enhancers/carriers in medical diagnostics and analytical biochemistry, solubilizers for various materials, as well as their role as a support matrix for chemical ingredients and as penetration enhancers in cosmetic products.

More recent developments have reported on the field of liposomal drugs, from the viewpoint of clinically approved products, with cancer therapy representing the main area of interest [34,35]. In this context, liposomes can be used to improve current cancer treatment regimens due to their capacity to increase the solubility of poorly water-soluble antitumor drugs. Moreover, these also act to decrease the mononuclear phagocyte system's (MPS) uptake by using long-circulating liposomes which promote a passive directing toward the tumor region and can lead to an active directing toward the tumor site by connecting specific ligands to the liposome surface [36]. These strategies minimize drug degradation and inactivation upon administration, as well as increase the drug's bioavailability and the fraction of drug delivered within the pathological area, thus improving efficacy and/or minimizing drug toxicity.

Alongside, in cancer chemotherapy, liposome as nanomedicine has a special interest, it enables the preferential delivery of drugs to the tumoral site, introducing the concept of *Enhanced Permeability and Retention* (EPR) effect, a particular phenomenon of solid tumors as a result of their anatomical and physiopathological characteristics that makes them different from normal tissues (Fig. 4). The endothelial cells from malignant blood vessels present larger gaps than normal blood vessel junctions (5–10 nm), that range from 100 nm to several hundred nanometres between them. In consequence, solid tumors exhibit selective extravasation and retention of drug-loaded liposomes. Moreover, these liposomes are cleared by the lymphatics in healthy tissues. However, in solid tumors most of these lymphatic vessels are collapsed and compressed, therefore the liposomes are selectively retained [37]. Ideally, nanocarriers, such as micelles or liposomes, by virtue of their size, can escape from the vasculature through the leaky endothelium overlying the tumor and then accumulating preferentially in solid tumors [38].

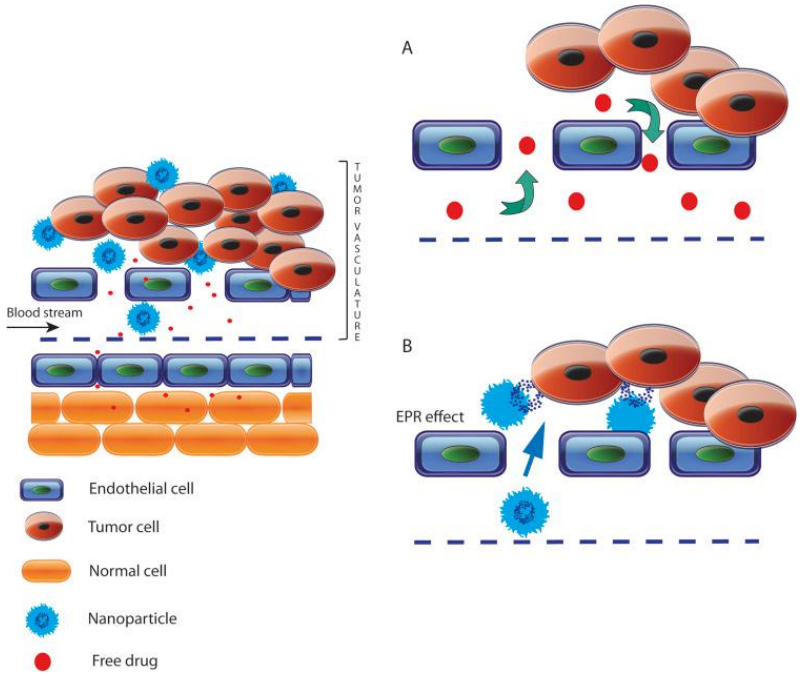

Figure 4. Schematic representation of enhanced permeability and retention (EPR) effect. Typical blood vessels from solid tumor contain pores of various sizes,

which allow nanoparticles and molecules of drug to enter into the interstitium of tumor tissue. (A) However, due to their small size, anticancer drugs can diffuse freely in and out of the tumor site, hence, only low levels of the drug accumulate in tumor. At the same time, significant concentrations of the agent are found in normal tissues. (B) The size of nanoparticles allows them to extravasate through gaps into the extravascular spaces and accumulate inside the tumor where the carrier releases the drug. (Bernabeu, Ezequiel, et al. International journal of pharmaceutics 526.1-2 (2017): 474-495).[39]

- **Definition and structure of liposomes**

Liposomes are spherical vesicles composed of one or more lipid bilayers, involving an aqueous compartment (Figure 5). These are formed spontaneously when the lipids are dispersed in an aqueous medium by stirring, in turn giving rise to a population of vesicles which may reach a size range from dozens of nanometres to dozens of microns in diameter [40]. The lipid molecules possess head groups which are attracted to water molecules and organize themselves in such a way as to point toward the aqueous cavity, whereas the hydrocarbon tails are repelled by the water molecules and point in the opposite direction.

The head groups of the inner layer point in the direction of the intravesicular fluid, with the tails pointing away from it. As such, the hydrocarbon tails of one layer point toward the hydrocarbon tails of the outer layer, in turn forming the normal bilipid membrane [35]. Once the liposomes have reached both the aqueous and lipid phases, they can encapsulate drugs with widely varying lipophilicities in the lipid bilayer, in the entrapped aqueous volume, or at the bilayer interface [41].

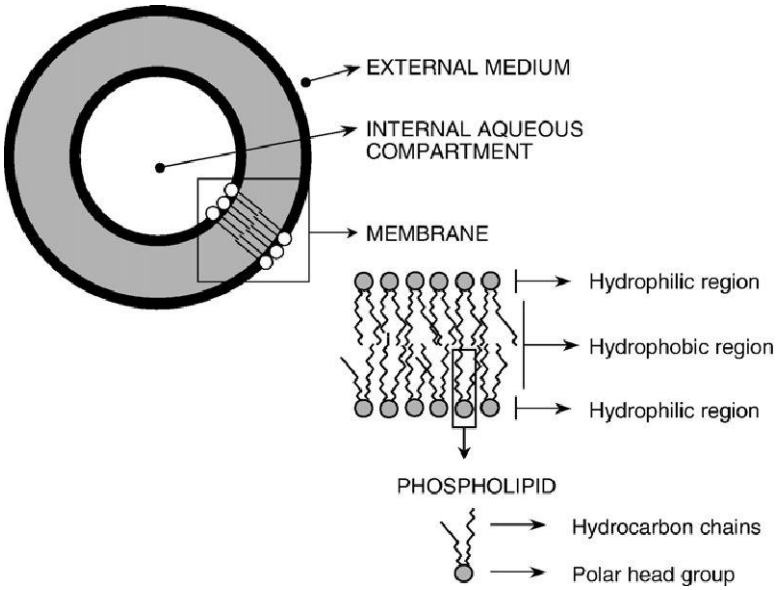

Figure 5. Basic structure and composition of liposomes. (Frézard, Frédéric, Neila M. Silva-Barcellos, and Robson AS dos Santos. Regulatory peptides 138.2-3 (2007): 59-65.) [42]

- **Liposome Composition**

Liposomes are composed mainly of natural and/or synthetic phospho- and sphingo-lipids with other membrane bilayer constituents, such as cholesterol and hydrophilic polymer conjugated lipids positioned randomly around each liposomal vesicle [43]. Phosphatidylcholine (PC; also known as lecithin) and phosphatidylethanolamine (PE) are the most common phospholipid found in both plants and animals and constitute the major structural parts of biologic membranes [44]. In contrast, the membranes of liposomes and other lipid- based drug delivery systems consist mostly of PC with little PE present [44]. This is because PE has the ability to form non-bilayer structures under physiologic conditions, destabilize membranes, and induce membrane fusion [45]. Other phospholipids, such as phosphatidylserine (PS), phosphatidylglycerol (PG), and phosphatidylinositol (PI), can also be used in the preparation of liposomes, depending on the desired liposomal characteristics [44].

Cholesterol is also an important component in the preparation of liposomes. Once it is incorporated into the liposomal membrane bilayer, cholesterol arranges itself among the phospholipid molecules with its hydroxyl group facing toward the water phase, whereas its tetracyclic ring inserts itself between the first few carbons of the fatty acyl chains into the hydrocarbon core of the membrane bilayer [44]. The incorporation of cholesterol into liposomes helps to decrease the fluidity of the liposomal membrane bilayer, reduce the permeability of water soluble molecules through the liposomal membrane, and improve the stability of the liposomal membrane in biologic fluids, such as blood and plasma [44]. In the absence of cholesterol, liposomes often interact with blood proteins, such as albumin, transferrin, macroglobulin, and high density lipoprotein [43,44,46]. These proteins tend to destabilize liposomes, and thus, decrease their capacity as a drug delivery system [46]. Although cholesterol has the ability to protect liposomes from being destabilized by blood proteins, the loss of liposomal phospholipids cannot be prevented completely [46].

Apart from cholesterol, a small fraction of polymers containing hydrophilic groups, especially polyethylene glycol (PEG), are at times conjugated to the surface of liposomes. PEG is often used for its stealth functions in nanoparticle formulations because it is a hydrophilic and flexible polymer [47]. The conjugation of PEG to the surface of the liposomal phospholipid bilayer reduces the interaction of liposomes with plasma proteins through steric hindrance [48,49]. As a result, this prevents plasma proteins, such as opsonin, from adsorbing to the surface of liposomes, which reduces opsonization and uptake of liposomes by the reticuloendothelial system (RES) [48]. The conjugation of PEG or PEGylation allows liposomes to circulate within the body for a longer period of time, extending their circulation half-life and, consequently, increasing the accumulation of liposomes within tumors [49].

- **Methods of liposomes preparation**

As mentioned before, liposomes are spontaneously formed when phospholipids are hydrated. Additional steps are often necessary to modify the size distribution and lamellarity of liposomes. Liposome preparation involves three major steps: vesicle formation, vesicle size reduction, and purification. Several preparation methods have been established based on the scale of the production and other considerations, such as drug encapsulation efficiency, the drug's physicochemical characteristics, and the administration route.

The most commonly used methods for liposome preparation are lipid hydration and the replacement of organic solvents by an aqueous media (reverse-phase evaporation and organic-solvent injection). The lipid hydration followed by vortex or manual stirring, also known as Bangham's method, consists of dissolving the lipids in a suitable organic solvent, such as chloroform or methanol [50]. This process is then followed by removing the solvent under reduced pressure, by rotary evaporation, until a thin film has been formed. After, the thin film is hydrated in an aqueous medium, above the phase-transition temperature, resulting in the formation of MLV liposomes (Figure 6). This is the simplest method of vesicle formation; however, it is limited in use due to its low encapsulation ability [51].

All methods based on the replacement of an organic solvent by an aqueous media show that the solvents, whether miscible or immiscible with water, are replaced by an aqueous solution. First, the water-immiscible organic solution containing lipids is injected into the aqueous phase (reverse-phase method), or the stepwise addition of the organic phase (specifically, ethanol) is injected into the aqueous phase (organic solvent injection method), followed by the removal of the solvent. These methods are able to form liposomes with a high encapsulation percentage of both hydrophilic and lipophilic substances. Generally, the incorporation of lipophilic drugs is

performed through their co-dissolution with the lipids [51]. Hydrophilic drugs are dissolved in the aqueous medium, whereas amphiphilic drugs can be dissolved in both mediums. The processes of liposome preparation can result in the formation of large vesicles (MLV) with heterogeneous size distribution; therefore, it is important to calibrate the formulation using a vesicle size reduction method.

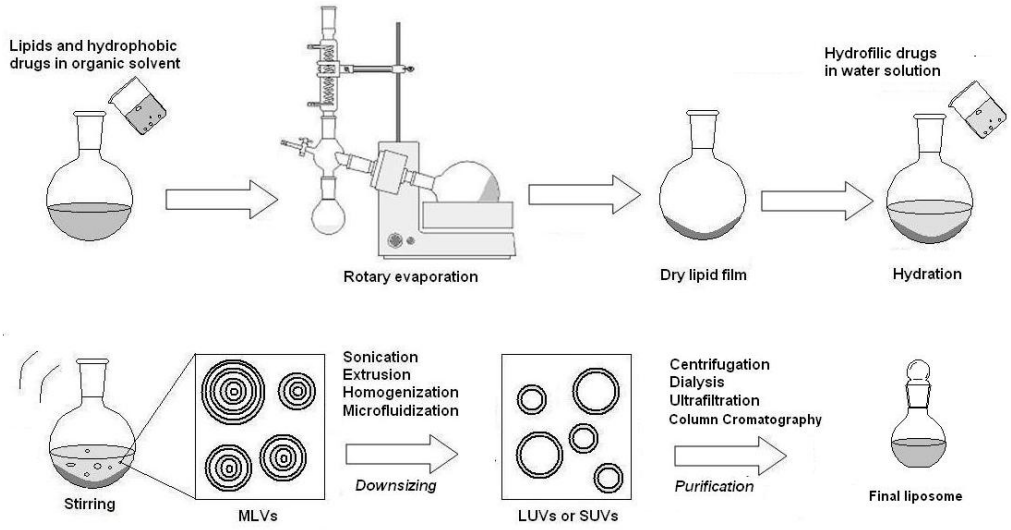

Figure 6. Representation of liposome production by lipid hydration followed by vortex or manual stirring. (Lopes, S.; Giuberti, C.; Rocha, T.; Ferreira, D.; Leite, E.; Oliveira, M. Conv. Innov. Approaches -b. 2013, 85–124) [52]

- **Characterization of liposomes**

The behaviour of liposomes in storage conditions and biological mediums is determined by specific factors, such as the size and surface charge of vesicles, chemical composition, membrane permeability, quantity of entrapped solutes, as well as the quality and purity of raw materials. Thus, it is of utmost importance to have as much information as possible regarding these parameters [40].

Bilayer constituents are responsible for the shelf-life; interactions with biological components, such as specific tissues, cells, and proteins; as well as the kinetics of the release of the entrapped drug in liposomes. The size of the liposomes influences it's *in vivo* distribution, as this factor can determine the amount of time that the liposomes will remain in the bloodstream before being removed. By contrast, the surface charge of vesicles influences their physical stability due to the possible occurrence of fusion and/or aggregation phenomena [40]. Therefore, detailed chemical, physical, and physicochemical characterizations are important in an attempt to ensure the efficacy and stabilization of the liposome formulation.

Physical characterization consists of determining the size, surface charge, and lamellarity of the liposomes. As the performance of liposomes *in vivo* and physical stability strongly depend on the vesicle size, liposome size distribution should be determined during the preparation process and storage. On the other hand, the nature and density of the charge on the liposome surface are important parameters that influence the mechanism and extent of liposome-cell interaction. Furthermore, the retention of the superficial charge for long periods during storage contributes to the high physical stability of the formulation

References

1. Siegel, R.L.; Miller, K.D.; Jemal, A. Cancer statistics, 2018. *CA. Cancer J. Clin.* **2018**, *68*, 7–30, doi:10.3322/caac.21442.

2. Howlader N, Noone AM, Krapcho M, Miller D, Bishop K, Kosary CL, Yu M, Ruhl J, Tatalovich Z, Mariotto A, Lewis DR, Chen HS, Feuer EJ, C.K. (eds). Cancer Statistics Review, 1975-2014 - SEER Statistics Available online: https://seer.cancer.gov/archive/csr/1975_2014/ (accessed on Jan 23, 2019).

3. Bell, D.A. Origins and molecular pathology of ovarian cancer. *Mod. Pathol.* **2005**, *18*, S19–S32, doi:10.1038/modpathol.3800306.

4. American Cancer Society *Cancer Facts & Figures 2018*; Atlanta, 2018;

5. Lister-Sharp, D.; McDonagh, M.S.; Khan, K.S.; Kleijnen, J. A rapid and systematic review of the effectiveness and cost-effectiveness of the taxanes used in the treatment of advanced breast and ovarian cancer. *Health Technol. Assess.* **2000**, *4*, 1–113.

6. Memarzadeh, S.; Berek, J.S. Advances in the management of epithelial ovarian cancer. *J. Reprod. Med.* **2001**, *46*, 621-9; discussion 629-30.

7. Rossof, A.H.; Talley, R.W.; Stephens, R.; Thigpen, T.; Samson, M.K.; Groppe, C.; Eyre, H.J.; Fisher, R. Phase II evaluation of cis-dichlorodiammineplatinum(II) in advanced malignancies of the genitourinary and gynecologic organs: a Southwest Oncology Group Study. *Cancer Treat. Rep. 63*, 1557–64.

8. Thigpen, T.; Shingleton, H.; Homesley, H.; LaGasse, L.; Blessing, J. cis-Dichlorodiammineplatinum(II) in the treatment of gynecologic malignancies: phase II trials by the Gynecologic Oncology Group. *Cancer Treat. Rep. 63*,

1549–55.

9. Decker, D.G.; Fleming, T.R.; Malkasian, G.D.; Webb, M.J.; Jeffries, J.A.; Edmonson, J.H. Cyclophosphamide plus cis-platinum in combination: treatment program for stage III or IV ovarian carcinoma. *Obstet. Gynecol.* **1982**, *60*, 481–7.

10. Piccart, M.J.; Bertelsen, K.; James, K.; Cassidy, J.; Mangioni, C.; Simonsen, E.; Stuart, G.; Kaye, S.; Vergote, I.; Blom, R.; et al. Randomized intergroup trial of cisplatin-paclitaxel versus cisplatin-cyclophosphamide in women with advanced epithelial ovarian cancer: three-year results. *J. Natl. Cancer Inst.* **2000**, *92*, 699–708.

11. McGuire, W.P.; Hoskins, W.J.; Brady, M.F.; Kucera, P.R.; Partridge, E.E.; Look, K.Y.; Clarke-Pearson, D.L.; Davidson, M. Cyclophosphamide and Cisplatin Compared with Paclitaxel and Cisplatin in Patients with Stage III and Stage IV Ovarian Cancer. *N. Engl. J. Med.* **1996**, *334*, 1–6, doi:10.1056/NEJM199601043340101.

12. Wani, M.C.; Taylor, H.L.; Wall, M.E.; Coggon, P.; McPhail, A.T. Plant antitumor agents. VI. The isolation and structure of taxol, a novel antileukemic and antitumor agent from Taxus brevifolia. *J. Am. Chem. Soc.* **1971**, *93*, 2325–7.

13. Wall, M.E.; Wani, M.C. Camptothecin and taxol: discovery to clinic--thirteenth Bruce F. Cain Memorial Award Lecture. *Cancer Res.* **1995**, *55*, 753–60.

14. SCHIFF, P.B.; FANT, J.; HORWITZ, S.B. Promotion of microtubule assembly in vitro by taxol. *Nature* **1979**, *277*, 665–667, doi:10.1038/277665a0.

15. Malawista, S.E.; Bensch, K.G. Human polymorphonuclear leukocytes:

demonstration of microtubules and effect of colchicine. *Science* **1967**, *156*, 521–2, doi:10.1126/SCIENCE.156.3774.521.

16. Kops, G.J.P.L.; Weaver, B.A.A.; Cleveland, D.W. On the road to cancer: aneuploidy and the mitotic checkpoint. *Nat. Rev. Cancer* **2005**, *5*, 773–785, doi:10.1038/nrc1714.

17. Waters, J.C.; Chen, R.H.; Murray, A.W.; Salmon, E.D. Localization of Mad2 to kinetochores depends on microtubule attachment, not tension. *J. Cell Biol.* **1998**, *141*, 1181–91, doi:10.1083/JCB.141.5.1181.

18. Weiss, R.B.; Donehower, R.C.; Wiernik, P.H.; Ohnuma, T.; Gralla, R.J.; Trump, D.L.; Baker, J.R.; Van Echo, D.A.; Von Hoff, D.D.; Leyland-Jones, B. Hypersensitivity reactions from taxol. *J. Clin. Oncol.* **1990**, *8*, 1263–8, doi:10.1200/JCO.1990.8.7.1263.

19. Gelderblom, H.; Verweij, J.; Nooter, K.; Sparreboom, A. Cremophor EL: the drawbacks and advantages of vehicle selection for drug formulation. *Eur. J. Cancer* **2001**, *37*, 1590–1598, doi:10.1016/S0959-8049(01)00171-X.

20. Singla, A.K.; Garg, A.; Aggarwal, D. Paclitaxel and its formulations. *Int. J. Pharm.* **2002**, *235*, 179–192, doi:10.1016/S0378-5173(01)00986-3.

21. Panchagnula, R. Pharmaceutical aspects of paclitaxel. *Int. J. Pharm.* **1998**, *172*, 1–15, doi:10.1016/S0378-5173(98)00188-4.

22. Gianni, L.; Kearns, C.M.; Giani, A.; Capri, G.; Viganó, L.; Lacatelli, A.; Bonadonna, G.; Egorin, M.J. Nonlinear pharmacokinetics and metabolism of paclitaxel and its pharmacokinetic/pharmacodynamic relationships in humans. *J. Clin. Oncol.* **1995**, *13*, 180–90, doi:10.1200/JCO.1995.13.1.180.

23. Wiernik, P.H.; Schwartz, E.L.; Strauman, J.J.; Dutcher, J.P.; Lipton, R.B.;

Paietta, E. Phase I clinical and pharmacokinetic study of taxol. *Cancer Res.* **1987**, *47*, 2486–93.

24. Rowinsky, E.K.; Donehower, R.C. Paclitaxel (Taxol). *N. Engl. J. Med.* **1995**, *332*, 1004–1014, doi:10.1056/NEJM199504133321507.

25. Sonnichsen, D.S.; Relling, M. V. Clinical Pharmacokinetics of Paclitaxel. *Clin. Pharmacokinet.* **1994**, *27*, 256–269, doi:10.2165/00003088-199427040-00002.

26. Sparreboom, A.; van Zuylen, L.; Brouwer, E.; Loos, W.J.; de Bruijn, P.; Gelderblom, H.; Pillay, M.; Nooter, K.; Stoter, G.; Verweij, J. Cremophor EL-mediated alteration of paclitaxel distribution in human blood: clinical pharmacokinetic implications. *Cancer Res.* **1999**, *59*, 1454–7.

27. Wall, M.E. Camptothecin and taxol: Discovery to clinic. *Med. Res. Rev.* **1998**, *18*, 299–314, doi:10.1002/(SICI)1098-1128(199809)18:5<299::AID-MED2>3.0.CO;2-O.

28. Marupudi, N.I.; Han, J.E.; Li, K.W.; Renard, V.M.; Tyler, B.M.; Brem, H. Paclitaxel: a review of adverse toxicities and novel delivery strategies. *Expert Opin. Drug Saf.* **2007**, *6*, 609–621, doi:10.1517/14740338.6.5.609.

29. Scripture, C.; Figg, W.; Sparreboom, A. Peripheral Neuropathy Induced by Paclitaxel: Recent Insights and Future Perspectives. *Curr. Neuropharmacol.* **2006**, *4*, 165–172, doi:10.2174/157015906776359568.

30. Legha, S.S.; Tenney, D.M.; Krakoff, I.R. Phase I study of taxol using a 5-day intermittent schedule. *J. Clin. Oncol.* **1986**, *4*, 762–6, doi:10.1200/JCO.1986.4.5.762.

31. Shigehiro, T.; Kasai, T.; Murakami, M.; Sekhar, S.C.; Tominaga, Y.; Okada, M.; Kudoh, T.; Mizutani, A.; Murakami, H.; Salomon, D.S.; et al. Efficient drug

delivery of paclitaxel glycoside: A novel solubility gradient encapsulation into liposomes coupled with immunoliposomes preparation. *PLoS One* **2014**, *9*, doi:10.1371/journal.pone.0107976.

32. Mandai, T.; Okumoto, H.; Oshitari, T.; Nakanishi, K.; Mikuni, K.; Hara, K. ji; Hara, K. zo; Iwatani, W.; Amano, T.; Nakamura, K.; et al. Synthesis and biological evaluation of water soluble taxoids bearing sugar moieties. *Heterocycles* **2001**, *54*, 561–566.

33. Mandai, T.; Okumoto, H.; Oshitari, T.; Nakanishi, K.; Mikuni, K.; Hara, K.; Hara, K. A Practical Synthetic Method for a- and b-Glycosyloxyacetic Acids. *Heterocycles* **2000**, *52*, 129, doi:10.3987/COM-99-S43.

34. Malam, Y.; Loizidou, M.; Seifalian, A.M. Liposomes and nanoparticles: nanosized vehicles for drug delivery in cancer. *Trends Pharmacol. Sci.* **2009**, *30*, 592–599, doi:10.1016/J.TIPS.2009.08.004.

35. Raffa, V.; Vittorio, O.; Riggio, C.; Cuschieri, A. Progress in nanotechnology for healthcare. *Minim. Invasive Ther. Allied Technol.* **2010**, *19*, 127–135, doi:10.3109/13645706.2010.481095.

36. Torchilin, V. Multifunctional and stimuli-sensitive pharmaceutical nanocarriers. *Eur. J. Pharm. Biopharm.* **2009**, *71*, 431–444, doi:10.1016/J.EJPB.2008.09.026.

37. Wang, A.Z.; Langer, R.; Farokhzad, O.C. Nanoparticle Delivery of Cancer Drugs. *Annu. Rev. Med.* **2012**, *63*, 185–198, doi:10.1146/annurev-med-040210-162544.

38. Maeda, H.; Bharate, G.Y.; Daruwalla, J. Polymeric drugs for efficient tumor-targeted drug delivery based on EPR-effect. *Eur. J. Pharm. Biopharm.* **2009**, *71*, 409–419, doi:10.1016/J.EJPB.2008.11.010.

39. Bernabeu, E.; Cagel, M.; Lagomarsino, E.; Moretton, M.; Chiappetta, D.A. Paclitaxel: What has been done and the challenges remain ahead. *Int. J. Pharm.* **2017**, *526*, 474–495, doi:10.1016/J.IJPHARM.2017.05.016.

40. New, R.R.C. *Characterization of liposomes. Liposomes: A practical*; Oxford University Press: New York, 1990;

41. Lasic, D.D. Novel applications of liposomes. *Trends Biotechnol.* **1998**, *16*, 307–321, doi:10.1016/S0167-7799(98)01220-7.

42. Frézard, F.; Silva-Barcellos, N.M.; Dos Santos, R.A.S. A novel approach based on nanotechnology for investigating the chronic actions of short-lived peptides in specific sites of the brain. **2006**, doi:10.1016/j.regpep.2006.11.021.

43. Sharma, A.; Sharma, U.S. Liposomes in drug delivery: Progress and limitations. *Int. J. Pharm.* **1997**, *154*, 123–140, doi:10.1016/S0378-5173(97)00135-X.

44. Vemuri, S.; Rhodes, C.. Preparation and characterization of liposomes as therapeutic delivery systems: a review. *Pharm. Acta Helv.* **1995**, *70*, 95–111, doi:10.1016/0031-6865(95)00010-7.

45. Ellens, H.; Bentz, J.; Szoka, F.C. Destabilization of phosphatidylethanolamine liposomes at the hexagonal phase transition temperature. *Biochemistry* **1986**, *25*, 285–294, doi:10.1021/bi00350a001.

46. Kirby, C.; Gregoriadis, G. The effect of the cholesterol content of small unilamellar liposomes on the fate of their lipid components in vivo. *Life Sci.* **1980**, *27*, 2223–2230, doi:10.1016/0024-3205(80)90388-4.

47. Bergström, K.; Osterberg, E.; Holmberg, K.; Hoffman, A.S.; Schuman, T.P.; Kozlowski, A.; Harris, J.H. Effects of branching and molecular weight of surface-bound poly(ethylene oxide) on protein rejection. *J. Biomater. Sci.*

Polym. Ed. **1994**, *6*, 123–32.

48. Allen, T.M.; Ryan, J.L.; Papahadjopoulos, D. Gangliosides reduce leakage of aqueous-space markers from liposomes in the presence of human plasma. *Biochim. Biophys. Acta - Biomembr.* **1985**, *818*, 205–210, doi:10.1016/0005-2736(85)90571-1.

49. Allen, C.; Dos Santos, N.; Gallagher, R.; Chiu, G.N.C.; Shu, Y.; Li, W.M.; Johnstone, S.A.; Janoff, A.S.; Mayer, L.D.; Webb, M.S.; et al. Controlling the physical behavior and biological performance of liposome formulations through use of surface grafted poly(ethylene glycol). *Biosci. Rep.* **2002**, *22*, 225–50, doi:10.1023/A:1020186505848.

50. Bangham, A.D. *LIPID BILAYERS AND BIOMEMBRANES*; 1972;

51. Wagner, A.; Vorauer-Uhl, K. Liposome technology for industrial purposes. *J. Drug Deliv.* **2011**, *2011*, 591325, doi:10.1155/2011/591325

CHAPTER 2

CD44 As Target Receptor

CD44

CD44, the lymphocyte homing receptor, as described by [1], attracted considerable interest when it was first described that expression of splice variants of the molecule suffice to confer the metastatic phenotype to locally growing tumour cells [2]. There is ample evidence for the importance of CD44 expression in the progression of many tumour types, as well as for its expression on cancer-initiating cells (CICs; also known as cancer stem cells, CSCs)

CSCs have been defined as a selected population of tumour cells that grow on serial transplantation in xenogeneic models. These assays revealed that CSCs can self-renew, and that tumours derived from purified CSCs recapitulate the heterogeneous phenotype of the parental. tumour, reflecting the differentiation capacity of CSCs [3–5]. CSCs, like stem cells, are highly resistant to apoptosis and are thought to be essential for metastasis formation after prolonged dormancy [5]. Distinct from stem cells, CSCs might not be genetically stable [6] and can be heterogeneous [7] .

- **The structure of CD44**

CD44 was cloned in 1989 and identified as a member of the cartilage link protein family [8]. CD44 is an important receptor that binds hyaluronan (HA) [9]. CD44 glycoproteins, which are encoded by a single gene [10], vary in size owing to N-glycosylation and O-glycosylation [8] and the insertion of alternatively spliced exon products in the extracellular domains of the molecule [10]. The smallest, standard or haematopoietic isoform (CD44s) is present on the membrane of most vertebrate cells [11]. CD44 has seven extracellular domains, a transmembrane domain and a cytoplasmic domain [12]. The cytoplasmic domain can be encoded

by exons 9 or 10 (Ref. [13]). Between domains 5 and 6, up to ten variant exon products can be inserted by alternative splicing [10] (Fig. 1).

The five amino-terminal exons encode a globular structure that contains two binding domains, the link domain (amino acids 32–132) and a basic motif outside the link domain (amino acids 150–158) to which HA binds [9]. Binding sites within the globular structure for collagen, laminin [14], fibronectin [15] and cell surface receptors such as CD62E and CD62L [16] have also been characterized. CD44 has two active binding sites for other glycosaminoglycans (GAGs)22. Four conserved cysteines are important for the stability of the extracellular domain, and two cysteines in the flanking region are important for correct folding of the link domain [17]. Between the N-terminal globular domain and the transmembrane domain there is a stretch of 46 amino acids that form a stalk-like structure [18]. This structure contains putative proteolytic cleavage sites and is heavily glycosylated [19]. This stretch can be enlarged by the insertion of variable exon products [20]. O-glycosylation and the cytoplasmic tail of CD44 can affect membrane subdomain localization and so influence the interaction of CD44 with HA [21].

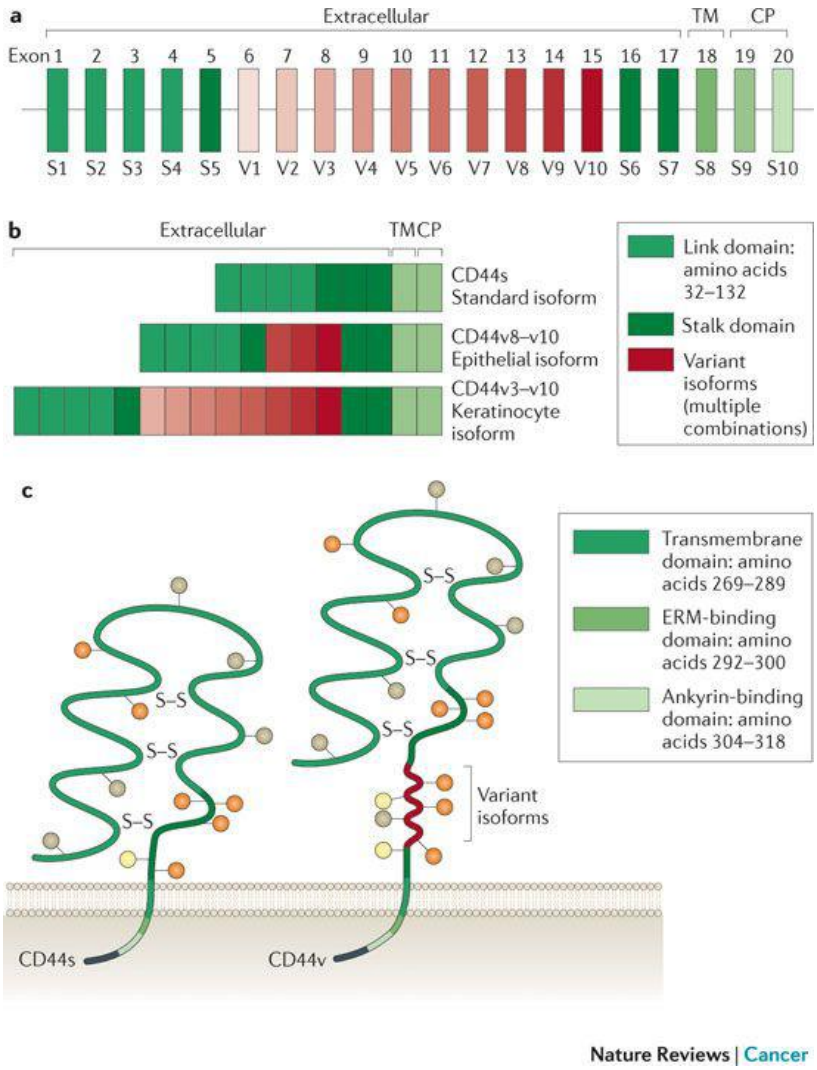

Figure 1. (a) CD44 consists of several exons, some of which are constant region exons that are used in every CD44 mRNA and protein (green bars) and others are variant exons (red bars) that are used in the CD44 variant proteins and are selected by alternative splicing. (b) Examples of alternatively spliced CD44 proteins. (c)The CD44 protein is composed of an extracellular link domain, a stalk-like region in the extracellular domain close to the transmembrane region, where the variant exon products (red) are inserted, the transmembrane region (TM) and the cytoplasmic tail (CP). There are multiple sites for N-glycosylation (brown circles) and O-glycosylation (orange circles) and two active glycosaminoglycan (GAG)-binding sites (yellow circles), one located in the v3 exon product. The link module contains the binding site for hyaluronan (HA). The cytoplasmic tail has binding motifs for

cytoskeletal linker proteins, as well as for SRC kinases. ERM, ezrin, radixin and moesin; S–S, disulphide bonds. (Zöller, M. *Nat. Rev. Cancer* **2011**, *11*, 254–267) [22]

- **CD44 as target receptor**

As mentioned before CD44 has been identified as one of the most established and common biomarkers associated with CSCs that exhibit highly malignant and chemo-resistant properties in a variety of tumors. CD44 is also expressed on hemopoietic, epithelial, and neuronal cells at low levels and known to participate in a wide variety of cellular functions including regulation of cell adhesion, proliferation, migration, growth, survival, angiogenesis, differentiation, and matrix-cell signalling processes in collaboration with other cellular proteins [23]. Clinical studies have shown a positive correlation between expression of CD44 and the tumor biological behaviors such as prognosis, tumor genesis growth and metastasis [22]. These findings stress the importance of CD44 as a potential attractive receptor for therapeutic targeting especially in tumors over expressing CD44 [24].

Among different strategies, antibody-based cancer treatments represent the major anti-CSC approach [25]. It has been shown that anti-CD44 antibodies can inhibit tumor progression and induce differentiation or apoptosis of leukemic cells [26]. Other studies showed that activating anti-CD44 monoclonal antibody (MAb) induces CD44 signalling, which can cause apoptosis [27] and suppress leukemic CSCs [28]. Based on this concept, we cultured hybridoma Hermes-3 cells (HB-9480) to produce anti-hCD44 MAb. Anti-hCD44 MAb functioned as ligand to target CD44. Furthermore, this ligand would be bound to liposome encapsulated gPTX targeting CD44 positive ovarian cancer cells.

Result and Discussion

Anti-hCD44 MAb obtained from conditioned medium culturing HB-9480 cells. HB-9480 cells were adapted from normal medium (RPMI 1640 medium supplemented 10% FBS) to PFHM II medium, a serum free medium to get optimum purity of produced MAb. We could confirm the purity of produced Anti-hCD44 MAb from Figure 2 B. Two bands were appeared on fraction 1-5, first band was about 50 kDa and second band was about 28 kDa. Those are showed as heavy chain and light chain from IgG2a of Anti-hCD44 MAb. Western blot result of conditioned medium of HB-9480 cells culture for 0 to 10 days in Figure 1A, confirmed Anti-hCD44 MAb as mouse IgG with comparable protein expression more than 100 ng in 10 days culture. Prior to the result, we cultured HB-9480 cells in the bioreactor for 10 days. We could obtain 4-5 mg/ml in 1.5 -2 ml protein from 50 ml conditioned medium cultured 10 days.

Next, we evaluated the protein expression levels of CD44 positive and negative cancer cell lines detected by obtained of Anti-hCD44 MAb by western blot assay. This step could assessed whether our obtained MAb could detect or immuno-react to CD44 in cancer cells. We observed CD44 expression in the ovarian cancer cell lines SK-OV-3, OVCAR-3, and OVK18 (Figure 3A) and glioblastoma cell lines U251MG and U251MG-P1 (Figure 3B). Protein expression of CD44 detected by anti-hCD44 MAb, was found high in SK-OV-3, U251MG, U251MG-P1cells whereas was barely undetectable in OVCAR-3 and OVK18. The anti-hCD44 MAb showed the immunoreactive protein approximately at 85 kDa [29,30] which is attributed to the predominant isoform of CD44 known as the standard form. The presence of CD44+ within the SK-OV-3, U251MG, U251MG-P1cells were confirmed by flow cytometric analysis (Figure 3C). Since the expression of CD44 found consistent from western blot assay and flow cytometry assay, anti-hCD44

MAb was considered as suitable ligand to target CD44 in CD44 positive cancer cells.

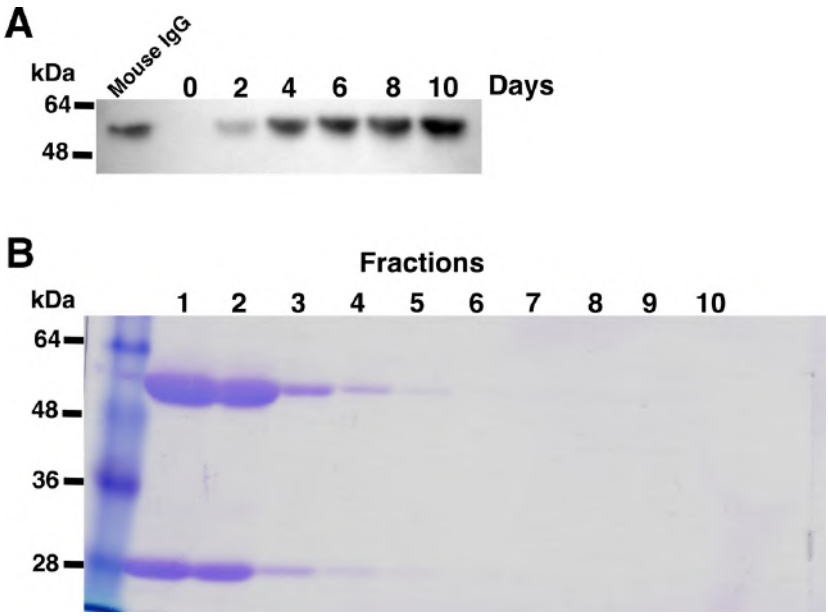

Figure 2. Anti-hCD44 MAb preparation. (A) Western blot result of conditioned medium of HB-9480 cells culture for 0 to 10 days detected by goat anti-mouse IgG-HRP (Santa Cruz Biotechnology Inc., CA, USA), 100 ng of Mouse IgG as positive control. (B) CBB staining of SDS PAGE of anti-hCD44 MAb eluted from protein A column.

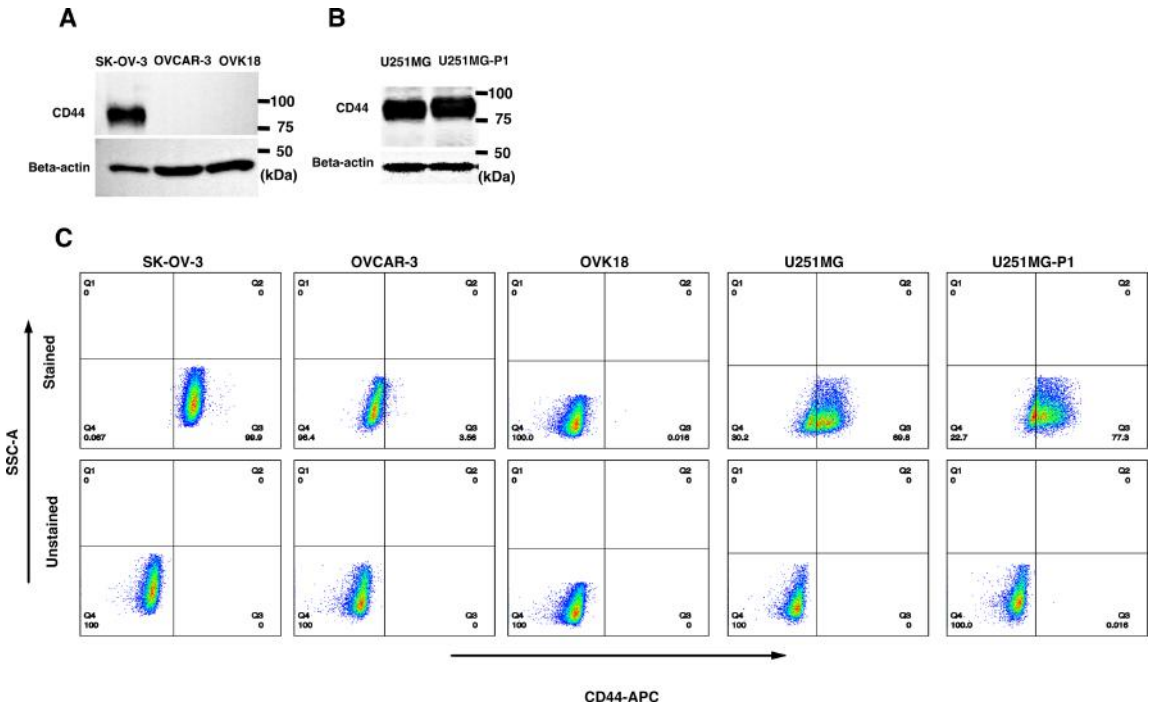

Figure 3. Anti-hCD44 MAb could detect CD44 protein expression in ovarian cancer and glioblastoma cells. Western blot analysis of human ovary cancer derived cells (A) and (B) human glioblastoma derived cells probed with anti-hCD44 MAb and human beta-actin antibody. (C) Cells contain $CD44^{+}$ population analyzed by flow cytometry by staining for CD44. The margins CD44 for each cell line were set up by non-stained cells as the negative control shown at the bottom of each analysis.

After conjugation to liposome encapsulated gPTX, the expression of anti-hCD44 confirmed in Figure 4. Further immunoliposome based drug delivery to CD44 positive cancer cells could be confirmed using anti-hCD44 MAb obtained as the ligand.

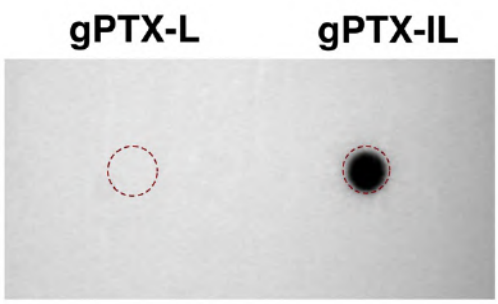

Figure 4. Dot blotting analysis of liposomes conjugated to ligands. Liposomes containing approximately 6 μg of gPTX in 2 μL were blotted onto PVDF membrane and probed with peroxidase-labelled Protein A (KPL, USA) (red dashed circle indicate the positions of dots). The immunoreactivity indicates that anti-hCD44 MAb was conjugated to liposome.

Materials and Method

- **Materials**

RPMI 1640 medium and DMEM were obtained from Sigma-Aldrich (St Louis, MO, *USA).*

- **Cells Culture and Experimental Animal**

The human ovarian cancer cell lines SK-OV-3 cells (HTB-77, ATCC, VA), OVK18 cells (TKG 0323, Cell Bank, Tohoku University, Sendai, Japan), and U251MG-P1 was isolated from a xenograft tumor of human glioblastoma cell line U251MG cells in mouse were cultured in DMEM medium supplemented with 10% fetal bovine serum (FBS) (Thermo Fisher Scientific, Waltham, MA, USA), containing 100 U/mL penicillin (Nacalai tesque, Kyoto, Japan), and 100 μg/mL streptomycin and OVCAR-3 (HTB-161, ATCC, VA) were cultured in RPMI 1640 medium supplemented with 10% FBS containing 100 U/mL penicillin, and 100 μg/mL streptomycin.

- **Preparation of anti-hCD44 MAb**

To produce anti-hCD44 MAb, hybridoma Hermes-3 cells (HB-9480, ATCC, VA) cells were cultured using a bioreactor, miniPERM (SARSTEDT, Nümbrecht, Germany). Twenty million of the cells were suspended in 50 mL of PFHM-II (Gibco, NY, USA) medium and were transferred into production module. The production module was connected to nutrient module containing 350 mL of PFHM-II. The bioreactor was rotated for 10 days at 37˚C in 5% CO2. The medium in production module was then collected and centrifuged at 150 xg for 5 min at 4˚C to remove the cells. The supernatant was re-centrifuged at 10,000 xg for 5 min at 4˚C. The supernatant was then passed through 0.20 μm filter (Sartorius Stedim Biotech GmBH, Geottingen, Germany) to completely remove cell debris. Anti-

hCD44 MAb was then purified as follows. The supernatant was passed through a 0.5 mL of Protein A Sepharose (GE Healthcare, Uppsala, Sweden) equilibrated with PBS. After washing the column with PBS, anti-hCD44 MAb was eluted using 0.1 M sodium-acetic buffer at pH 2.6. Five hundred µL of each fraction was readily neutralized with 10 µL of 2 M sodium phosphate buffer, pH 8.0. The fraction containing anti-hCD44 MAb was detected by western blotting using polyclonal anti mouse IgG HRP (DAKO, Denmark) and the protein concentration was determined using a BCA assay kit (Pierce Biotechnology, Rockford, IL, USA).

- **Expression of CD44 in Ovarian Cancer Cells line.**

  - ***Western blotting***

Proteins following the SDS-PAGE were transferred to polyvinylidene difluoride (PVDF) membranes (Merck Millipore, Burlington, MA, USA). To detect CD44 epitope, the blot was probed using anti-hCD44 MAb (2 mg/mL, 1:2000) followed by polyclonal anti-mouse IgG HRP (1:4000) (DAKO, Denmark). Quantitative assessment of relative intensity of the blots were analyzed using ImageJ. The actin immunoreact to anti-beta actin Rabbit MAb (1:1000, 4970S, Cell Signalling Technology, Inc., Beverly, MA, USA) was used as a normalization control.

  - ***3.4.2 Flow cytometry analysis***

SK-OV-3, OVCAR-3, OVK18, U251MG, U251MG-P1 cells were harvested at logarithmic growth phase, followed by being re-suspended in 100ul PBS, stained with APC labelled mouse anti-human CD44 MAb (BD Science Pharmingen, San Diego, CA, USA) and analyzed by BD AccuriTM C6 plus flow cytometer (Becton & Dickinson, Franklin Lakes, NJ, USA). Data of each experiment was analyzed using FlowJo software (FlowJo, LLC, Ashland, OR, USA).

References

1. Gallatin, W.M.; Weissman, I.L.; Butcher, E.C. A cell-surface molecule involved in organ-specific homing of lymphocytes. *Nature 304*, 30–4.

2. Günthert, U.; Hofmann, M.; Rudy, W.; Reber, S.; Zöller, M.; Hauβmann, I.; Matzku, S.; Wenzel, A.; Ponta, H.; Herrlich, P. A new variant of glycoprotein CD44 confers metastatic potential to rat carcinoma cells. *Cell* **1991**, *65*, 13–24, doi:10.1016/0092-8674(91)90403-L.

3. Fábián, Á.; Barok, M.; Vereb, G.; Szöllősi, J. Die hard: Are cancer stem cells the Bruce Willises of tumor biology? *Cytom. Part A* **2009**, *75A*, 67–74, doi:10.1002/cyto.a.20690.

4. Sales, K.M.; Winslet, M.C.; Seifalian, A.M. Stem Cells and Cancer: An Overview. *Stem Cell Rev.* **2007**, *3*, 249–255, doi:10.1007/s12015-007-9002-0.

5. Allan, A.L.; Vantyghem, S.A.; Tuck, A.B.; Chambers, A.F. Tumor Dormancy and Cancer Stem Cells: Implications for the Biology and Treatment of Breast Cancer Metastasis. *Breast Dis.* **2007**, *26*, 87–98, doi:10.3233/BD-2007-26108.

6. Conway, A.E.; Lindgren, A.; Galic, Z.; Pyle, A.D.; Wu, H.; Zack, J.A.; Pelligrini, M.; Teitell, M.A.; Clark, A.T. A Self-Renewal Program Controls the Expansion of Genetically Unstable Cancer Stem Cells in Pluripotent Stem Cell-Derived Tumors. *Stem Cells* **2009**, *27*, 18–28, doi:10.1634/stemcells.2008-0529.

7. Adams, J.M.; Strasser, A. Is Tumor Growth Sustained by Rare Cancer Stem Cells or Dominant Clones? *Cancer Res.* **2008**, *68*, 4018–4021, doi:10.1158/0008-5472.CAN-07-6334.

8. Stamenkovic, I.; Amiot, M.; Pesando, J.M.; Seed, B. A lymphocyte molecule implicated in lymph node homing is a member of the cartilage link protein

family. *Cell* **1989**, *56*, 1057–1062, doi:10.1016/0092-8674(89)90638-7.

9. Aruffo, A.; Stamenkovic, I.; Melnick, M.; Underhill, C.B.; Seed, B. CD44 is the principal cell surface receptor for hyaluronate. *Cell* **1990**, *61*, 1303–1313, doi:10.1016/0092-8674(90)90694-A.

10. Screaton, G.R.; Bell, M. V; Jackson, D.G.; Cornelis, F.B.; Gerth, U.; Bell, J.I. Genomic structure of DNA encoding the lymphocyte homing receptor CD44 reveals at least 12 alternatively spliced exons. *Proc. Natl. Acad. Sci. U. S. A.* **1992**, *89*, 12160–4, doi:10.1073/PNAS.89.24.12160.

11. Naor, D.; Wallach-Dayan, S.B.; Zahalka, M.A.; Sionov, R.V. Involvement of CD44, a molecule with a thousand faces, in cancer dissemination. *Semin. Cancer Biol.* **2008**, *18*, 260–267, doi:10.1016/J.SEMCANCER.2008.03.015.

12. Idzerda, R.L.; Carter, W.G.; Nottenburg, C.; Wayner, E.A.; Gallatin, W.M.; St John, T. Isolation and DNA sequence of a cDNA clone encoding a lymphocyte adhesion receptor for high endothelium. *Proc. Natl. Acad. Sci. U. S. A.* **1989**, *86*, 4659–63, doi:10.1073/PNAS.86.12.4659.

13. Goldstein, L.A.; Butcher, E.C. Identification of mRNA that encodes an alternative form of H-CAM(CD44) in lymphoid and nonlymphoid tissues. *Immunogenetics* **1990**, *32*, 389–97.

14. Ishii, S.; Ford, R.; Thomas, P.; Nachman, A.; Steele, G.; Jessup, J.M. CD44 participates in the adhesion of human colorectal carcinoma cells to laminin and type IV collagen. *Surg. Oncol.* **1993**, *2*, 255–64.

15. Jalkanen, S.; Jalkanen, M. Lymphocyte CD44 binds the COOH-terminal heparin-binding domain of fibronectin. *J. Cell Biol.* **1992**, *116*, 817–25.

16. Konstantopoulos, K.; Thomas, S.N. Cancer Cells in Transit: The Vascular

Interactions of Tumor Cells. *Annu. Rev. Biomed. Eng.* **2009**, *11*, 177–202, doi:10.1146/annurev-bioeng-061008-124949.

17. Greenfield, B.; Wang, W.C.; Marquardt, H.; Piepkorn, M.; Wolff, E.A.; Aruffo, A.; Bennett, K.L. Characterization of the heparan sulfate and chondroitin sulfate assembly sites in CD44. *J. Biol. Chem.* **1999**, *274*, 2511–7, doi:10.1074/JBC.274.4.2511.

18. Screaton, G.R.; Bell, M. V; Bell, J.I.; Jackson, D.G. The identification of a new alternative exon with highly restricted tissue expression in transcripts encoding the mouse Pgp-1 (CD44) homing receptor. Comparison of all 10 variable exons between mouse, human, and rat. *J. Biol. Chem.* **1993**, *268*, 12235–8.

19. Okamoto, I.; Kawano, Y.; Murakami, D.; Sasayama, T.; Araki, N.; Miki, T.; Wong, A.J.; Saya, H. Proteolytic release of CD44 intracellular domain and its role in the CD44 signaling pathway. *J. Cell Biol.* **2001**, *155*, 755–62, doi:10.1083/jcb.200108159.

20. Kalniņa, Z.; Zayakin, P.; Siliņa, K.; Line, A. Alterations of pre-mRNA splicing in cancer. *Genes Chromosom. Cancer* 2005, *42*, 342–357.

21. Neame, S.J.; Isacke, C.M. The cytoplasmic tail of CD44 is required for basolateral localization in epithelial MDCK cells but does not mediate association with the detergent-insoluble cytoskeleton of fibroblasts. *J. Cell Biol.* **1993**, *121*, 1299–310, doi:10.1083/JCB.121.6.1299.

22. Zöller, M. CD44: can a cancer-initiating cell profit from an abundantly expressed molecule? *Nat. Rev. Cancer* **2011**, *11*, 254–267, doi:10.1038/nrc3023.

23. Ponta, H.; Sherman, L.; Herrlich, P.A. CD44: From adhesion molecules to signalling regulators. *Nat. Rev. Mol. Cell Biol.* **2003**, *4*, 33–45,

doi:10.1038/nrm1004.

24. Naor, D.; Nedvetzki, S.; Golan, I.; Melnik, L.; Faitelson, Y. CD44 in Cancer. *Crit. Rev. Clin. Lab. Sci.* **2002**, *39*, 527–579, doi:10.1080/10408360290795574.

25. Deonarain, M.P.; Kousparou, C.A.; Epenetos, A.A. Antibodies targeting cancer stem cells: A new paradigm in immunotherapy? *MAbs* **2009**, *1*, 12–25, doi:10.4161/mabs.1.1.7347.

26. Liu, J.; Jiang, G. CD44 and Hematologic Malignancies. *Cell. Mol. Immunol.* **2006**, *3*, doi:10.1111/coin.12024.

27. Song, G.; Liao, X.; Zhou, L.; Wu, L.; Feng, Y.; Han, Z.C. HI44a, an anti-CD44 monoclonal antibody, induces differentiation and apoptosis of human acute myeloid leukemia cells. *Leuk. Res.* **2004**, *28*, 1089–1096, doi:10.1016/J.LEUKRES.2004.02.005.

28. Jin, L.; Hope, K.J.; Zhai, Q.; Smadja-Joffe, F.; Dick, J.E. Targeting of CD44 eradicates human acute myeloid leukemic stem cells. *Nat. Med.* **2006**, *12*, 1167–1174, doi:10.1038/nm1483.

29. Ween, M.P.; Oehler, M.K.; Ricciardelli, C. Role of versican, hyaluronan and CD44 in ovarian cancer metastasis. *Int. J. Mol. Sci.* **2011**, *12*, 1009–1029, doi:10.3390/ijms12021009.

30. Xu, Y.; Stamenkovic, I.; Yu, Q. CD44 attenuates activation of the Hippo signaling pathway and is a prime therapeutic target for glioblastoma. *Cancer Res.* **2010**, *70*, 2455–2464, doi:10.1158/0008-5472.CAN-09-2505.

CHAPTER 3

Targeting Ovarian Cancer Cells Overexpressing CD44 with Immunoliposomes Encapsulating Glycosylated Paclitaxel

LIST OF ABBREVIATIONS AND ACRONYMS

PTX	Paclitaxel
gPTX	Glycosylated Paclitaxel
anti-hCD44 MAb	Anti-human CD44 Monoclonal Antibody
gPTX-L	Glycosylated Paclitaxel-Liposome
gPTX-IL	Glycosylated Paclitaxel-Immunoliposome (anti-hCD44 MAb)
FAM	6-Carboxyfluorescein
FAM-L	6-Carboxyfluorescein -Liposome
FAM-IL	6-Carboxyfluorescein-Immunoliposome (anti-hCD44 MAb)
CEP	Cremophore, Ethanol, PBS
CEP-IL	Cremophore, Ethanol, PBS-Immunoliposome (anti-hCD44 MAb)
PBS	Phosphate Buffer Saline

ABSTRACT

Paclitaxel (PTX) is one of the front-line drugs approved for the treatment of ovarian cancer. However, the application of PTX is limited due to the significant hydrophobicity and poor pharmacokinetics. We previously reported target-directed liposomes carrying tumor-selective conjugated antibody and encapsulated glycosylated PTX (gPTX-L) which successfully overcome the PTX limitation. The tubulin stabilizing activity of gPTX was equivalent to that of PTX while the cytotoxic activity of gPTX was reduced. In human ovarian cancer cell lines, SK-OV-3 and OVK18, the IC_{50} for gPTX range 15-20 nM, which was sensitive enough to address gPTX-L with tumor-selective antibody coupling for ovarian cancer therapy. The cell membrane receptor CD44 is associated with cancer progression and has been recognized as a cancer stem cell marker including ovarian cancer, becoming a suitable candidate to be targeted by gPTX-L therapy. In this study, gPTX-loading liposomes conjugated with anti-CD44 antibody (gPTX-IL) were assessed for the efficacy of targeting CD44-positive ovarian cancer cells. We successfully encapsulated gPTX into liposomes with the loading efficiency more than 80% in both of gPTX-L and gPTX-IL with a diameter of approximately 100 nm with efficacy of enhanced cytotoxicity *in vitro* and of convenient treatment *in vivo*. As the result, gPTX-IL efficiently suppressed tumor growth *in vivo*. Therefore gPTX-IL could be a promising formulation for effective ovarian cancer therapies. .

Introduction

Ovarian cancer ranks the eighth cause of cancer death in women worldwide and annually estimated 151,900 in 238,700 of new cases[2]. In the US as one of the typical developed countries, it ranks the fifth cause of lethal tumors among women, accounting for the seriousness in female gynecological cancers[1]. The standard treatment of progressive ovarian cancer is surgical resections followed by systemic chemotherapy[3,4]. The National Comprehensive Cancer Network (NCCN) guideline shows the first line of chemotherapy for ovarian cancer encompasses administration of carboplatin, paclitaxel (PTX), or the administration of these two.

PTX acts as an anti-cancer agent preventing cells division by promoting and stabilizing the assembly of microtubule structures[4–6]. Because PTX is highly hydrophobic, the mixture of Cremophor EL® and ethanol has been adopted as solvent for the commercial formulation known as Taxol. However, Cremophor EL® may induce anaphylactoid and/or anaphylactic reactions *in vivo*[7]. Taxol treatment itself is followed by side effects such as hypersensitivity reactions, nephrotoxicity and neurotoxicity[8,9]. Therefore, these disadvantages of Taxol treatment should urgently be ameliorated by the development of proper drug delivery system of PTX.

During the past half-century, liposome has been considered one of the most promising drug carrier system of PTX due to its versatility, intrinsic biocompatibility and potential variability[10]. The highly hydrophobic nature of PTX hinder the loading efficiency into the liposome to establish efficient liposomal formulation. Recently, we successfully developed liposomes encapsulating glycosylated paclitaxel (gPTX) in the hydrophilic-core[11]. gPTX is a PTX derivative with a glucose moiety coupled at the 7-OH radical[12], this modification enhanced the hydrophilicity of PTX allowing practically different solubility in the solvents CEP (Cremophor EL®, ethanol, and PBS; in 12:12:76 ratio) and EG (40% Ethylene Glycol). Exploiting the difference of

the solubility we could prepare stable gPTX liposome (gPTX-L) with sufficient amount of encapsulated drug. The outer layer of liposomes can be modified with coupled ligands targeting molecules localized on the cells membrane surface.

Active-targeting drug delivery with ligands as nanosystem have been utilized to optimize therapeutic efficacy and minimize systemic toxicity. Ligands for cell surface receptors highly expressed in tumor cell populations have provided a great specificity[13,14]. The cell membrane receptor CD44 could be one of the most promising candidates to be targeted[15–18]. CD44 is a receptor for hyaluronic acid type-1 transmembrane glycoprotein that is implicated in cell–cell and cell–matrix interactions and is associated with malignancy, particularly with metastasis promotion[19,20]. CD44 has also been considered as a cancer stem cell (CSC) marker in several malignancies of hematopoietic and epithelial origin[20], and is closely related with tumor progression and drug resistance[21–23] in several tumors including ovarian cancer[15,16]. Collectively, CD44 could be a suitable candidate target molecule in ovarian cancer to apply drug delivery and minimize side effects.

In this study, we improved preparation of gPTX-L to achieve higher encapsulation efficiency and designed gPTX-IL, gPTX-L bound to anti-human CD44 monoclonal antibody (anti-hCD44 MAb) to target CD44 overexpressing ovarian cancer cells evaluating the physical parameters of liposome and the efficacy of gPTX-IL targeting CD44 positive ovarian cancer cells.

Results

• Expression of CD44 in human ovarian cancer derived cells

First, we assessed the protein and mRNA expression levels of CD44 in the ovarian cancer cell lines SK-OV-3, OVCAR-3, and OVK18. Protein expression of CD44 detected by anti-hCD44 MAb, was found high in SK-OV-3 cells whereas was barely undetectable in OVCAR-3 and OVK18 (Figure 1A-B). The anti-hCD44 MAb showed the immunoreactive protein approximately at 85 kDa[24] (Figure 1 A), which is attributed to the predominant isoform of CD44 known as the standard form. The mRNA expression of CD44 by reverse transcription-polymerase chain reaction (qRT-PCR) shown in Figure 1C confirm the result of CD44 protein expression in the same manner. Since the overexpression of CD44 was only found in SK-OV-3 cells line, we considered it as representative of CD44-positive cells. Likewise, the anti-hCD44 MAb was considered as suitable ligand to target SK-OV-3 cells.

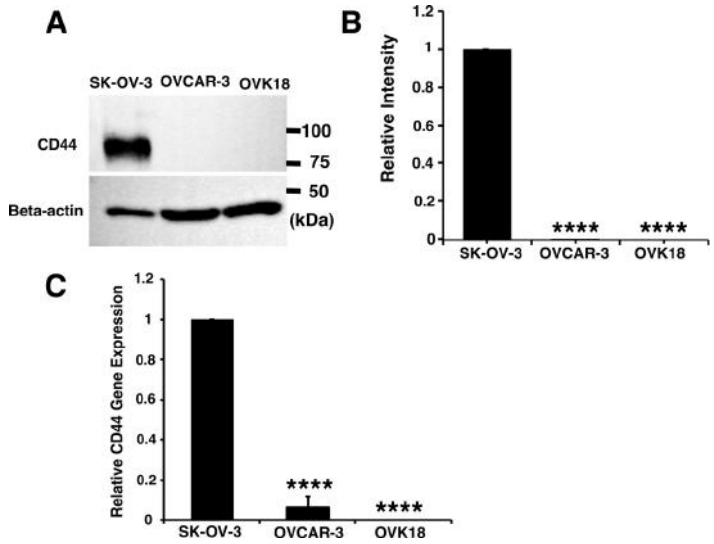

Figure 1. SK-OV-3 cells are overexpressing CD44. (A) Western blot analysis of human ovary cancer derived cells probed with anti-hCD44 MAb and human beta-actin antibody. (B) Relative intensity of the bands of CD44 to beta-actin in Western blot was densitometrically analyzed by ImageJ. (C)

Relative gene expression levels of CD44 to GAPDH were analyzed by rt-qPCR. The data presented as the mean ± SD from three independent experiments. The statistical significance in mean values of more than two groups was determined using one-way analysis of variance (ANOVA) and Dunnet multiple comparison test using CD44 expression of SK-OV-3 cells as control; (****) $p < 0.001$.

Next we confirmed the presence of $CD44^+$ within the SK-OV-3 cells. The SK-OV-3 cells were characterized by CD44 and CD24 through flow cytometric analysis being compared with OVCAR-3 and OVK18 cells. The expression two antigens CD44 and CD24 has recently been used to explain CSC population in breast cancer and ovarian cancer. The most population of SK-OV-3 cells exhibited $CD44^+$, consisting of both $CD44^+/CD24^-$ and $CD44^+/CD24^+$ population while OVK18 cells showed only $CD44^-/CD24^-$ population and OVCAR-3 cells showed most $CD44^-/CD24^+$ population (Figure 2).

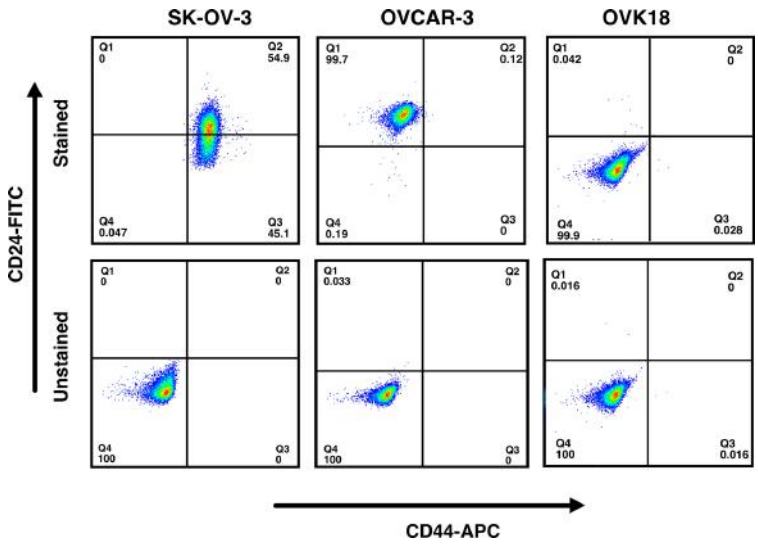

Figure 2. SK-OV-3 cells contain $CD44^+/CD24^-$ population as well as $CD44^+/CD24^+$ population. SK-OV-3, OVCAR-3, and OVK18 cells were analyzed by flow cytometry by staining for CD44 and CD24. The margins of

CD24 and CD44 for each cell line were set up by non-stained cells as the negative control shown at the bottom of each analysis. Most of the population in SK-OV-3 cells were found CD44 positive.

- **Sensitivity of human ovarian cancer derived cells to gPTX.**

We assessed the anticancer effect of gPTX toward SK-OV-3 cells as CD44 positive cells and OVK18 cells as CD44 negative cells. In our previous report, gPTX showed 3-fold weaker than PTX in breast cancer derived cells[11]. This observation was also consistent in ovarian cancer cells (Figure 3A-B). The reduced cytotoxicity should be caused by the increased of hydrophilicity of gPTX hindering penetration efficiency into the lipid bilayer of the cell membrane. However, IC_{50} value of gPTX toward both cell lines is in the range of 15-20 nM, which means the cells are sensitive enough to give feasibility of using gPTX for ovarian cancer treatment. Moreover, Encapsulation of gPTX into liposomes, which should confer gPTX with penetrability into cytoplasm, and specific ligand grafted on the liposome surface could help enhance the targeting potential minimizing systemic toxicity.

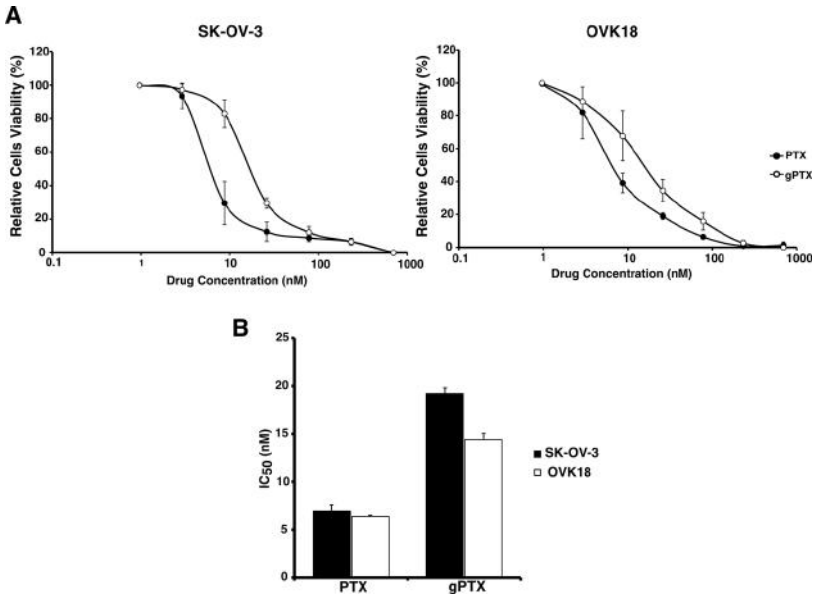

Figure 3. SK-OV-3 cells and OVK18 cells sensitive to paclitaxel and glycosylated paclitaxel. (A) PTX and gPTX sensitivity graph, cytotoxicity of both drug was assessed on SK-OV-3 and OVK18 cells by MTT assay after 72h drug treatment. (B) IC_{50} value of gPTX and PTX detemined by graph (A). The data presented as the mean ± SD from three independent experiment.

- **Potential uptake of liposome conjugated with anti-hCD44 MAb**

To assess the amount of anti-hCD44 MAb conjugated to the liposomes, we first prepared encapsulated 6-carboxyflourescent (FAM) into liposomes (FAM-L), which was conjugated with varying amount of anti-hCD44 MAb (FAM-IL) such as 5, 10, and 15 nmol/48 μmol DPPC, respectively. After 1h exposure of FAM-IL, flow cytometric analysis showed the population of SK-OV-3 cells stained with FAM were 52.7% by 5 nmol formulation, 52.9% by 10 nmol formulation, and 53.6% by 15 nmol formulation (Figure 4A). These results imply the efficiency of immunoliposome uptake should be related with receptor density on the cell surface but not on the ligand on liposome [25]. The minimum amount of 5 nmol appeared enough to prepare FAM-L providing no difference in the efficiency of uptake when compared with 10 and 15 nmol formulation. Based on the result, anti-hCD44 MAb was conjugated with gPTX-L at 5 nmol and 10 nmol/48 μmol DPPC while 15 nmol nmol formulation was not considered anymore because the amount of antibody was too much consuming. The IC_{50}s of the two formulations were assessed and 10 nmol formulation showed slightly lower IC_{50}, which was statistically significant than 5 nmol formulation (Figure 4B) We further tried the potential targeting of liposome by using anti-hCD44 MAb at 10 nmol formulation as same as amount that used in our previous reports yet by different ligands[11,18,26]

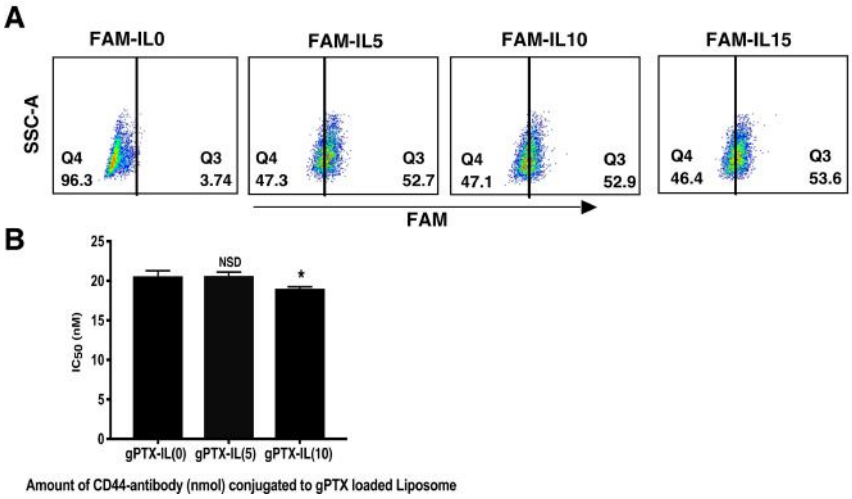

Figure 4. The uptake of liposomes conjugated with anti-hCD44 MAb was optimal at 10 nmol/48 μmol DPPC. (A) FAM-IL treatment with the amount of antibody varying from 5 to 15 nmol anti-hCD44 MAb in SK-OV-3 cells. Data are representative of three replicates. (B) IC50 of gPTX encapsulated in liposomes conjugating various amount of anti-hCD44 MAb against SK-OV-3 cells. The data presented as the mean ± SD (n = 3) from independent experiments. The statistical significance in mean values of more than two groups was determined using one-way analysis of variance (ANOVA) and Dunnett's multiple comparisons test were applied using gPTX-IL (0 nmol) as control, (*) $p < 0.05$; (NSD) no significant difference.

The targeting potential of the liposome conjugated with anti-hCD44 Mab 10 nmol formulation toward CD44 overexpressing cells, SK-OV-3, was further assessed by confocal microscopic observation and flow cytometric analysis. The green fluorescence intensity of FAM between FAM-L and FAM-IL was equivalent and the green fluorescence observed in the cytoplasmic area was correlated with the intracellular uptake levels of liposome. After 2 h incubation at 37˚C of FAM-L and FAM-IL in the culture of SK-OV-3 cells, the uptake of FAM was evaluated under confocal microscopy (Figure 5 A, B). Strong green fluorescent intensity of FAM was

observed in SK-OV-3 cells when exposed to FAM-IL. According to the validation by flow cytometric analysis, SK-OV-3 cells incorporated FAM-IL in 1 h and kept up to 3 h (Figure 5 C, D). In contrast, FAM-L did not show FAM fluorescence in OVK18 cells, which showed no expression of CD44. These results imply that immunoliposomes targeting CD44 could effectively enhance the cellular uptake as compared with non-targeted liposomes.

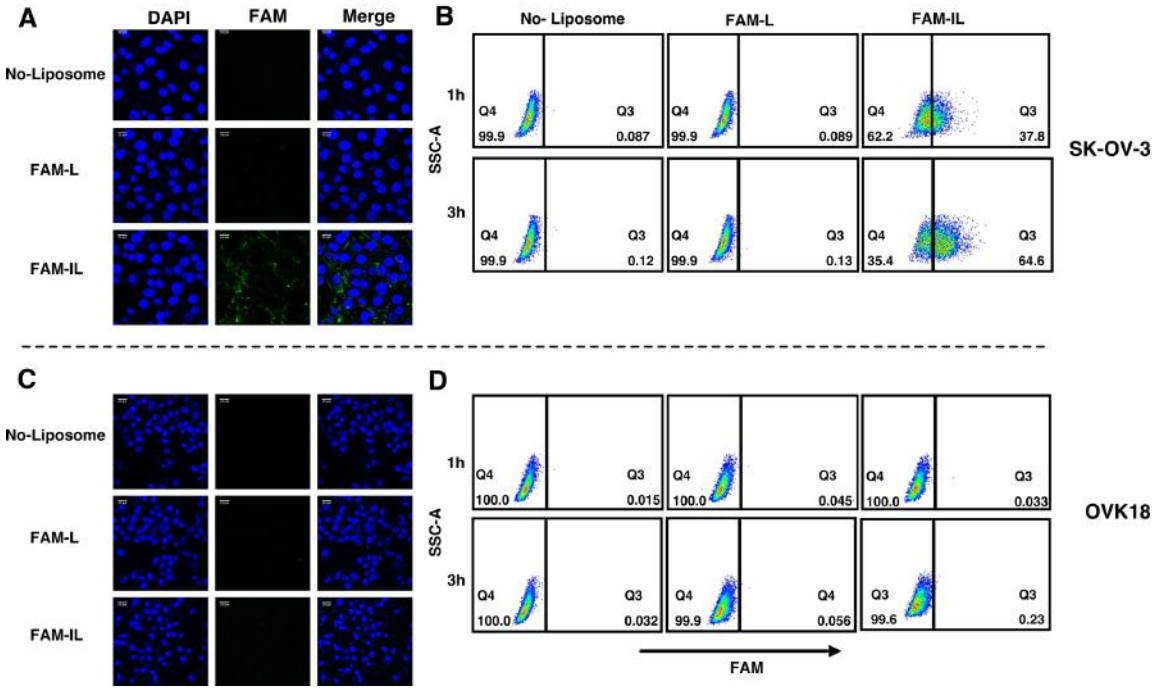

Figure 5. Immunoliposome enhanced cellular uptake in CD44 postive cells. (A,C) Confocal Microscopy image after 2h treatment FAM-L and FAM-IL. (B,D) Flow cytometry analysis after 1h and 3h treatment FAM-L and FAM-IL. FAM-L and FAM-IL were evaluated for the cellular uptake in SK-OV-3 (A,B) and OVK18 (C,D). Data are representative of three replicates.

- **Preparation and characterization of gPTX-L and gPTX-IL**

Preparation of liposomes encapsulating gPTX (gPTX-L) and those conjugated with anti-hCD44 MAb (gPTX-IL) followed the method previously described[11] except for the down-sizing procesure of liposomes. Liposomes containing CEP were

prepared by hydrating lipid film with CEP, which consisted of Cremophore, ethanol and PBS at the ratio of 12 : 12 : 76. Due to the high ratio of PBS, the hydrophobicity of CEP is not significant and we reported the similar ratio was sufficiently effective to encapsulate gPTX into liposomes, likewise CEP in our formula of liposome did not impair the stability of liposomes for 4 weeks after encapsulation of gPTX[11]. Then the liposomes encapsulated with gPTX were prepared by remote loading method to facilitate efficient encapsulation of gPTX into the inner aqueous core of liposomes. This method is exploiting the difference of solubility of gPTX in the two solvents, 40% EG and CEP. The gradient between the two solvents makes gPTX penetrate into liposomes efficiently because CEP increased the solubility of gPTX when compared with water and 40% EG. This remote loading process has previously been described as a driving force for active encapsulation of gPTX[11]. The down-sizing liposome process employed freeze-thawing process followed by extrusion through 100 nm polycarbonate membrane filter in place of sonication with a probe. We also modified gPTX-IL preparation by adding L-cysteine to block excess uncoupled maleimide[27,28]. We experienced this blockade was effective to stabilize gPTX-IL preventing drugs from leakage. We could successfully prepare both gPTX-IL and gPTX-L as nanoparticles with homogeneous diameters of approximately 100 nm with polydispersity indexes less than 0.3, with negative zeta potential, and an improved encapsulation efficiency of gPTX inside with/without anti-hCD44 MAb (70-90%). The characters for the liposomes encapsulating gPTX in this study are summarized in Table 1

Table 1. Characters of the liposomes encapsulating gPTX.

Formulation	Diameter (nm)	Polydispersity Index	Zeta Potential (-mV)	Encapsulation Efficiency (%)	Loading Efficiency (%)
gPTX-L	115±29	0.20±0.02	6.9±1.5	86.8±10.1	9.4±1.1
gPTX-IL	99.8±12	0.26±0.01	7.8±1.2	80.9±10.6	8.9±1.2
t-test	NSD	*	NSD	NSD	NSD

- Each experiment was performed in triplicate and the values are given as mean ± SD.
- The statistical significance in mean values between gPTX-L and gPTX-IL was performed by two-tailed students t-test. *, $p < 0.05$; NSD, no significant difference.

Both gPTX-L and gPTX-IL were observed under transmission electron microscopy (TEM) (Figure 6). The images consistently indicated the diameter of gPTX-IL and gPTX-L at around 100 nm as measured by dynamic light scattering and the shape of each particle was spherical with fairly smooth surface.

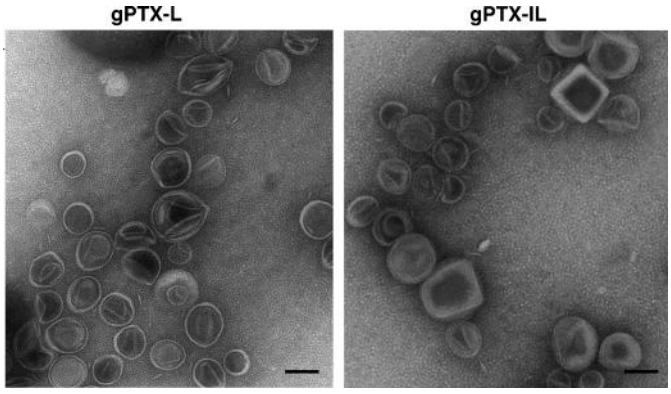

Figure 6. TEM images of liposome encapsulating gPTX. gPTX-IL showed unilamellar vesicles with diameter of approximately 100 nm similarly to gPTX-L . Each scale bar shows 100 nm.

- **Cytotoxicity of gPTX, gPTX-L, gPTX-IL *In Vitro***

First, we assessed IC_{50}s of gPTX as naked gPTX, gPTX-L, and gPTX-IL on SK-OV-3 and OVK18 cells comparing the two different exposure time 24 h (Figure 7A) and 72 h (Figure 7B). We found the exposure for 72 h of the three different formulations *in vitro* was too long to evaluate the IC_{50}s since liposomes would fuse with cellular membrane independent of the antibodies of immunoliposomes when exposure time was long enough. In this context, gPTX-IL feasibly showed the IC_{50} of 19 nM in SK-OV-3 cells while naked gPTX and gPTX-L showed IC_{50}s ranging in 20 to 22 nM, which were found in the small difference one another. To demonstrate the CD44 dependency of the immunoliposomes reducing the effect of the membrane fusion of liposomes, we thought that the drug exposure time should be shorter than 72 h. Antibody oriented targeting of gPTX-IL successfully observed to be accumulated on the surface of SK-OV-3 cells due to the affinity of the antibodies in 24h exhibiting the lowest IC_{50} of 23.4 nM while the IC_{50}s of gPTX-L and naked gPTX were ranging between 30 and 50 nM. These results suggest that gPTX-IL should target CD44-expressing cells more efficiently than gPTX-L. Meanwhile, in both cells, naked gPTX an gPTX-L were still cytotoxicic even though they do not have targeting ability. As for the cytotoxicity of naked gPTX, the molecule is possibly internalized into the cell via passive diffusion due to its poor hydrophilicity.

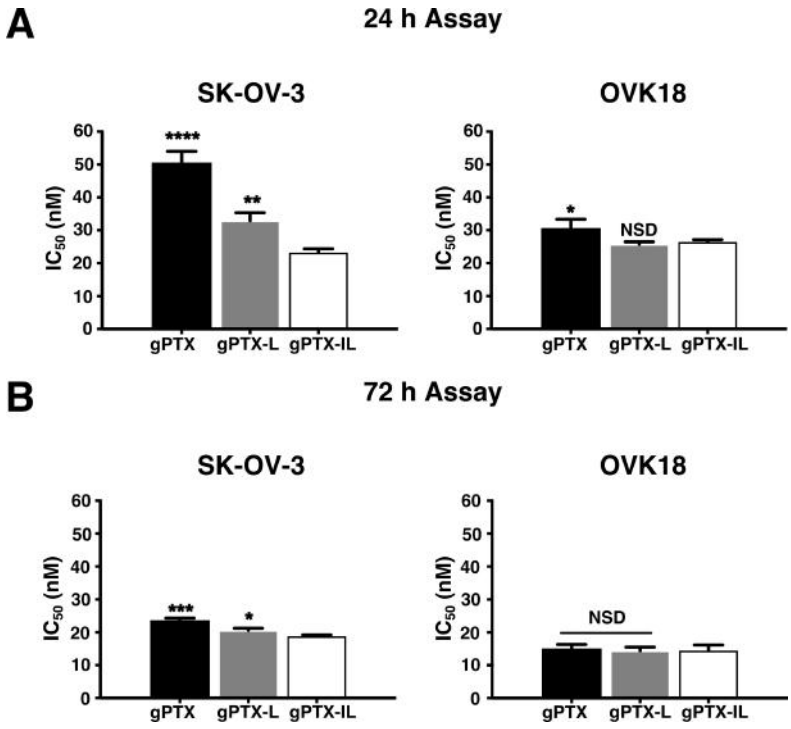

Figure 7. gPTX-IL exhibited the lowest inhibition concentration (IC_{50}) in SK-OV-3 cells. *In vitro* cytotoxicity IC_{50} of gPTX in different formulation after 24h (A) and 72 h (B) of exposure to SK-OV-3 cells and OVK18 cells was evaluated. The data presented as the mean ± SD (n = 3). The statistical significance in mean values of more than two groups was determined using one-way analysis of variance (ANOVA) and Dunnet multiple comparison test using IC_{50} value of gPTX-IL treatment as control, (*) $p < 0.05$; (**) $p < 0.01$; (***) $p < 0.005$; (****) $p < 0.001$; (NSD) no significant difference.

- **Suppression of tumor growth *In Vivo***

The suppression of tumor growth by gPTX-IL was evaluated in BALB/c nude mice bearing tumors of transplanted SK-OV-3 cells (Figure 8-10).

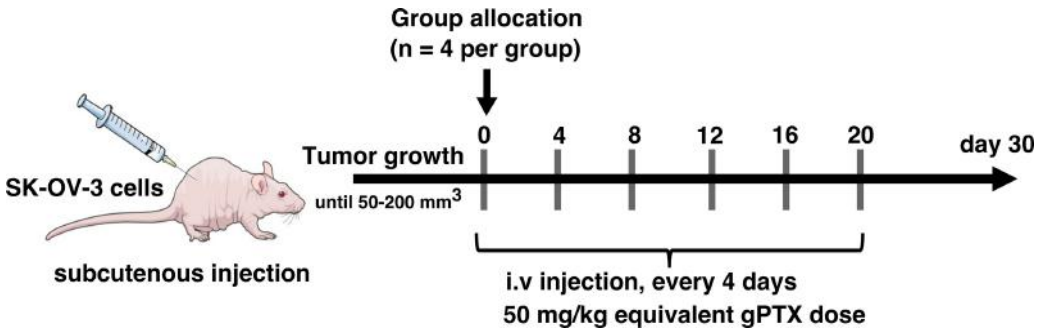

Figure 8. *In vivo* treatment scheme in BALB/C Nude mice bearing ovarian cancer of SK-OV-3 cells.

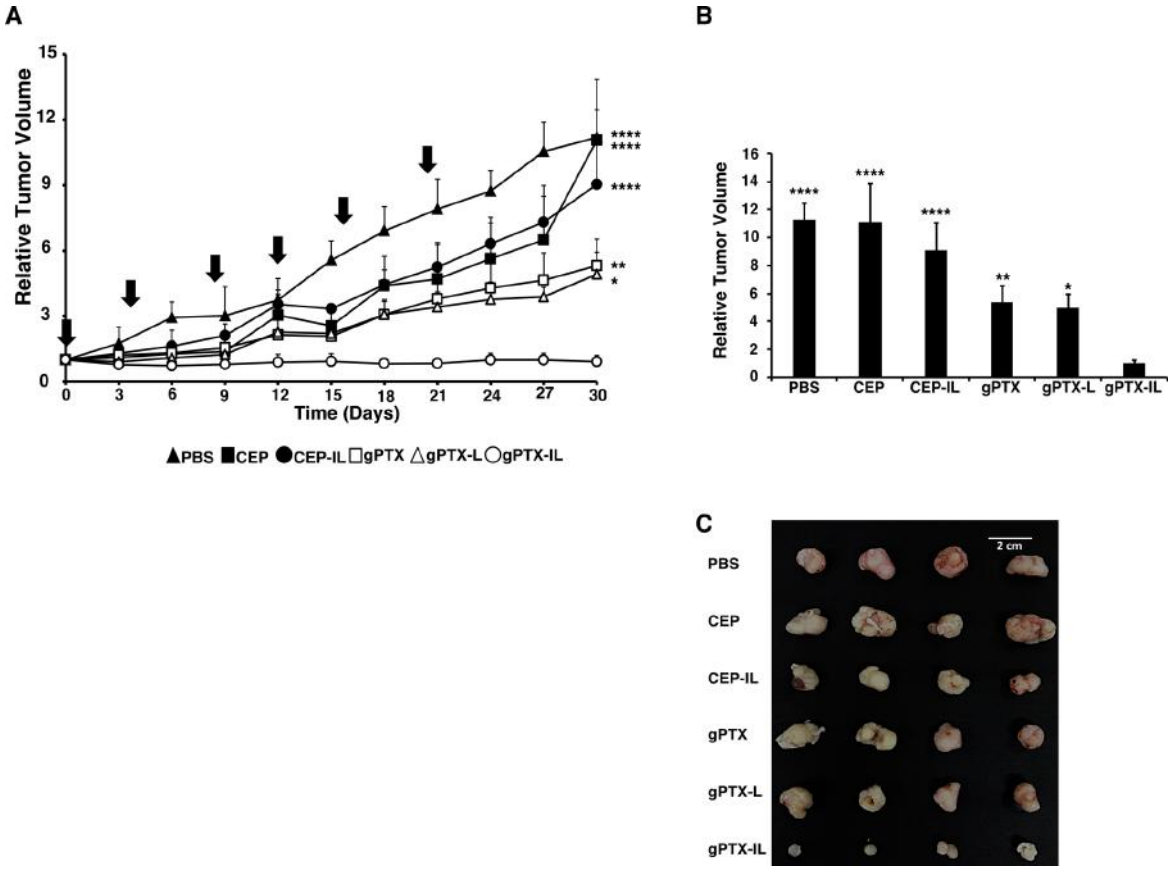

Figure 9. gPTX-IL suppressed tumor growth in the most effective manner *in vivo*. gPTX- IL (open circle), gPTX-L (open triangle), naked gPTX (open square), CEP-IL (closed circle), CEP (closed square), or PBS (cross) was intravenously injected at day 0, 4, 8, 12, 16, and 20 (indicated by vertical arrows). (A) The effect of different formulations of gPTX on the volume of tumors. (B) Relative tumor volume at day 30. gPTX-IL was the most effective

formulation to suppress the growth of tumor. The statistical significance in mean values of more than two groups was determined using one-way analysis of variance (ANOVA) and Dunnet multiple comparison test using relative tumor volume of gPTX-IL treatment as a control, (*) $p < 0.05$; (**) $p < 0.01$; (****) $p < 0.001$. (E) The tumors from the experiment (A) representing each group were displayed exhibiting the effect of each formulation of gPTX. Data are expressed as the mean with ±SD where n =4.

Naked gPTX, gPTX-L, and gPTX-IL were injected intravenously (i.v.) 6 times at the dose of 50 mg/kg of gPTX with 4-day intervals (Figure 9 and Figure 10). We were administered PBS, CEP, and CEP-IL as control. PBS as the vehicle of liposome, was injected in equivalence to the maximum volume of injected liposome. CEP as the solvent of naked gPTX, was injected in equivalence to the gPTX volume. CEP-IL as the representation of immunoliposome conjugated to anti-hCD44 MAb which encapsulates CEP alone, was injected based on the amount of lipid equivalent to that contained in gPTX-IL at dose 50 mg/kg. The tumor growth was observed for 30 days and the relative tumor volume was measured at every 3-day being normalized to the initial tumor volume at day 0. In our previous report, gPTX-IL conjugated to anti-HER2 MAb, was administered at 150 mg/kg as single dose injection in nude mice bearing HT-29 tumors and targeted with gPTX, it injected for 3 times in the 10 days interval [11]. This was an experiment to investigate the maximum tolerated dose to demonstrate effective high dose administration was possible.

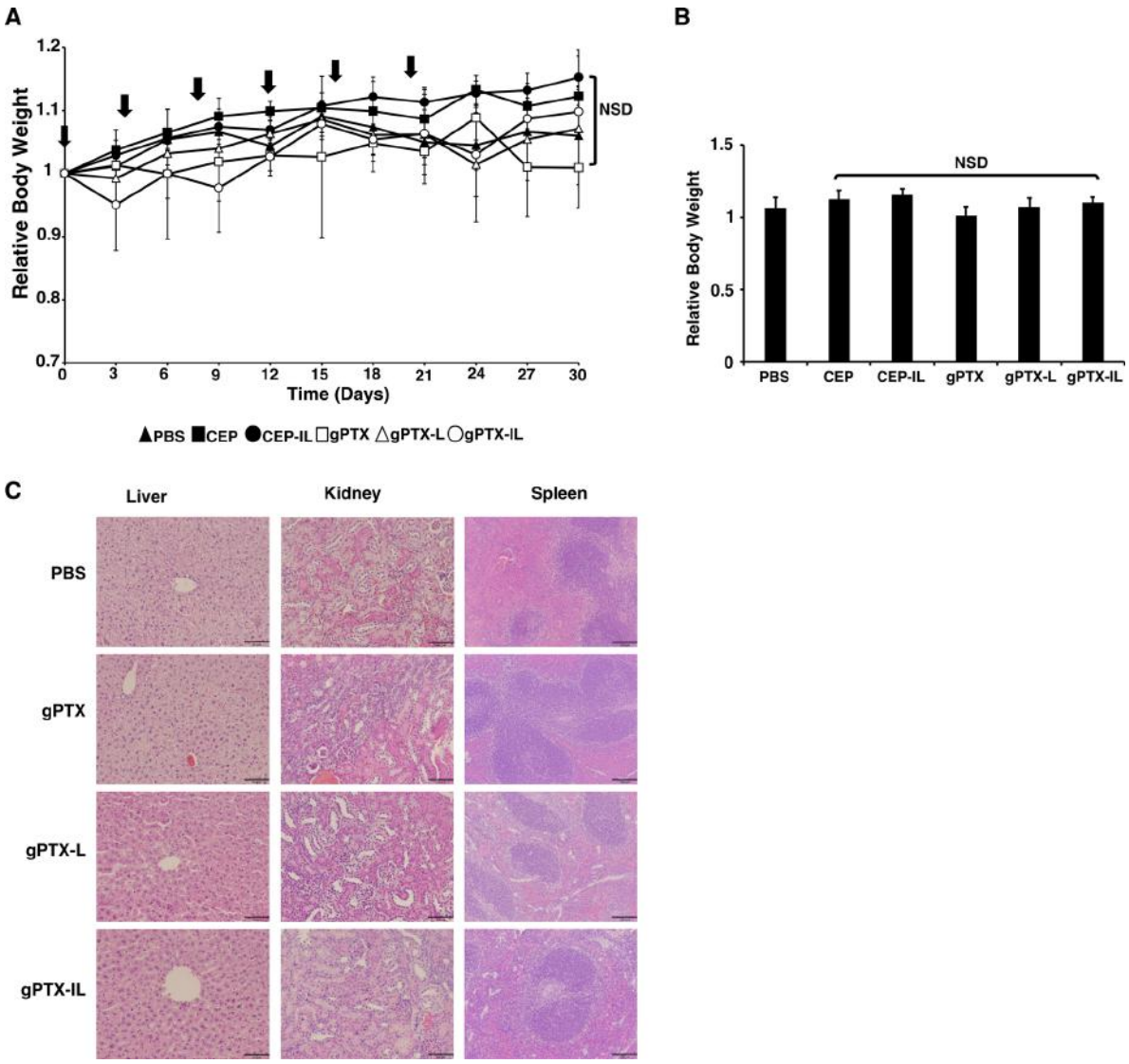

Figure 10. gPTX-IL treatment showed no significance side effects. gPTX- IL (open circle with line), gPTX-L (open triangle), naked gPTX (open square), CEP-IL (closed circle), CEP (closed square), or PBS (cross) was intravenously injected at day 0, 4, 8, 12, 16, and 20 (indicated by vertical arrows). (A) Change of body weight of mice bearing tumors. (B) Relative body weight at day 30. The statistical significance in mean values of more than two groups was determined using one-way analysis of variance (ANOVA) and Dunnet multiple comparison test using relative body weight of PBS treatment as a control, NSD, no significant difference. (C) H&E staining of some vital organs of the drug treated animal groups.

In contrast, we evaluated the effect of repeated i.v. injection of gPTX equivalent to 50 mg/kg in this study. All tumors from mice treated with five different formulations were excised at day 30 and were compared by tumor size and volume (Figure 9 A-C). Loss of body weight was not observed for any of the formulations (Figure 10 A,B). Moreover, pathological observation of liver, kidney, and spleen showed that gPTX-IL did not cause significant damage to the tissues during the experiment while naked drug and non-targeting liposome appeared to damage the tissues (Figure 10 C). In gPTX treatment, liver showed a cytoplasmic vacuolation. Simultaneously, kidney exhibited atrophied glomeruli and necrotic area. In addition, spleen had enlargement of lymphoid follicles of white pulp. In gPTX-L treatment, elongated trabeculus were found in spleen. Meanwhile, no damages were found in any of those tissues in gPTX-IL treatment. Of note, the tumor growth appeared completely suppressed solely by the administration of gPTX-IL. As a result , gPTX-IL showed excellent anti-tumor activity with less side effect.

Discussion

In this study, we designed a drug delivery system targeting ovarian cancer overexpressing CD44. CD44 is known as common CSC marker and considered critically related with the migration and adhesion of CSCs and during the formation of tumor tissue [20]. CSCs are thought to be resistant to chemotherapy and responsible for metastasis and recurrence. CD44 positive epithelial ovarian cancer stem cells were also found correlated with drug resistance and recurrence[22,29]. Therefore, we consider that the drug delivery targeting CD44 in ovarian cancer could lead to successful results in suppressing specifically CSC population in the tumor site. The screening of three ovarian cancer derived cell lines showed SK-OV-3 cells overexpressing CD44 while CD44 expression in OVCAR-3 and OVK18 cells was less or deficient (Figure 1). Consequently, SK-OV-3 cells were selected as the target of the drug delivery. Double staining of CD44 and CD24, which are both correlated with CSC markers, exhibited two different populations of $CD44^{+}/CD24^{-}$ and $CD44^{+}/CD24^{+}$ within SK-OV-3 cells, and only $CD44^{-}/CD24^{+}$ in OVCAR-3 cells and $CD44^{-}/CD24^{-}$ in OVK18 cells (Figure 2). The phenotype of $CD44^{+}/CD24^{-}$ in ovarian cancer cells has been reported to exhibit CSC-like properties of enhanced differentiation, invasion, and resistance to chemotherapy[30,31], while $CD44^{+}/CD24^{+}/Epcam^{+}$ exhibited stem cell characteristics in other report [32]. Therefore, SK-OV-3 cells display highly phenotype which should be a suitable candidate for the purpose to design drug delivery targeting CSC-like population in ovarian cancers.

In the present study, we successfully improve the encapsulation efficiency of both gPTX-L and gPTX-IL up to approximately 70-90% (Table 1) by replacing the process of down-sizing liposome from sonication to extrusion. The liposomes diameter, approximately 100 nm, of gPTX-L and gPTX-IL could be practical for the drug

delivery i.v. since particle size between 50 and 200 nm is considered sufficient for the accumulation of the drug in tumor via enhanced permeability and retention effect (EPR)[33].

The design of targeting CD44 is already employed to enhance drug efficacy and reduce systemic toxicity in ovarian cancer[34,35]. In this study, we employed anti-hCD44 MAb to design the liposome to target ovarian cancer. FAM-IL could successfully allow FAM uptake in the CD44 positive ovarian cancer in one hour exposure of FAM-IL (Figure 5). This result suggests that CD44-targeted liposomes involve receptor-mediated endocytosis with additional membrane fusion of lipid bilayers, resulting in a higher cellular uptake, as previously described that CD44 upregulation in the cancer cells assisted endocytosis via independent of clathrin-coated vesicles, the caveolae or macropinocytosis pathway[36–38]. As the result, gPTX-IL found to exhibit the most efficient target-oriented cytotoxicity in SK-OV-3 cells when compared to gPTX-L and naked gPTX in 24-hour treatment (Figure 7). We further evaluated the antitumor effects of gPTX-L and gPTX-IL *in vivo* with repeated administration at total dose of 300 mg/kg gPTX. gPTX-IL exhibited the most effective antitumor activity without side effect, which was evaluated by a loss of body weight and H&E staining of liver, kidney, and spleen (Figure 10). These results are consistent with those previously reported, liposome conjugated to anti-HER2 antibody efficiently accumulated and internalized into the HER2 positive cells in tumor tissue while non-targeting liposomes localized in the stroma [11,39]. In this context, gPTX-IL is conceivable superior to gPTX-L in the inhibition of tumor growth due to the retention time in tumor site.

We included CEP-IL as additional control in the *in vivo* experiment to see the role of CD44 antibody intrinsically, as stated antibody bound to empty liposome is able to improve the therapeutic efficacy and inhibit tumor growth even without cancer

drug[40]. CEP-IL did not show significant inhibition on tumor growth, although antigen dependent cellular cytotoxicity should be expected by the phagocytic activation of macrophages targeting the IgG molecule bound to antigens.

In summary, gPTX-IL was successfully demonstrated reduction of the tumor volume of the therapeutic efficacy against CD44-overexpressing ovarian cancer cells *in vivo*. Therefore, gPTX-IL should have a potential of advantageous strategy of drug delivery targeting cell surface molecules specific to ovarian cancer cells.

Conclusions

The cytotoxicity of gPTX, a derivative of PTX with a glucose moiety, exhibited the cytotoxicity equivalent to one fifth of the cytotoxicity by PTX against ovarian cancer derived cells. This cytotoxicity was considered due to the hydrophilicity from the glucose moiety. However, the IC_{50} of gPTX toward the cells was found still low enough to target ovarian cancer. Down-sizing of liposome by extruder and supplementing cysteine masking unreacted radicals improved the procedure of immunoliposome preparation to achieve practical encapsulation efficiency for gPTX-L and gPTX-IL. As the results, the preparation of sufficient quantities of both gPTX-L and gPTX-IL became practical.

gPTX-IL should quickly recognize the CD44 positive cancer cells and retain on the cell surface due to the antibody, implying that the potential of therapeutic effect should be high. As expected, gPTX-IL exhibited distinguished inhibition of tumor growth with less apparent side effects *in vivo*. Targeting CD44 in the ovarian cancer should be attributed to targeting CSC population, since overexpression of CD44 in SK-OV-3 could correlate with CSC–like character. Taking these into consideration, the immunoliposomes encapsulating practical amount of gPTX should be a promising formulation of anticancer drugs as a positive targeting drug delivery systems in ovarian cancer.

Materials and Methods

• Materials

Dipalmitoylphosphatidylcholine (DPPC), 1,2-distearoyl-sn-glycerol-3-phosphoethanolamine-N- [methoxy (polyethylene glycol)-2000] (mPEG–DSPE), and 1,2-distearoyl-sn-glycerol-3-phosphoethanolamine-N-[maleimide (polyethylene glycol)-2000] (Mal–PEG–DSPE) were obtained from NOF Co. (Tokyo, Japan). Cholesterol (Chol) was purchased from Kanto Chemical Co., Inc. (Tokyo, Japan). Thiazolyl blue tetrazolium bromide (MTT), RPMI 1640 medium and DMEM were obtained from Sigma-Aldrich (St Louis, MO, USA).). gPTX was synthesized as previously described[12].

• Cells Culture and Experimental Animal

The human ovarian cancer cell lines SK-OV-3 cells (HTB-77, ATCC, VA) and OVK18 cells (TKG 0323, Cell Bank, Tohoku University, Sendai, Japan) were cultured in DMEM medium supplemented with 10% fetal bovine serum (FBS) (Thermo Fisher Scientific, Waltham, MA, USA), containing 100 U/mL penicillin (Nacalai tesque, Kyoto, Japan), and 100 μg/mL streptomycin and OVCAR-3 (HTB-161, ATCC, VA) were cultured in RPMI 1640 medium supplemented with 10% FBS containing 100 U/mL penicillin, and 100 μg/mL streptomycin.

Four-week-old female BALB/c nude mice from Charles River (Kanagawa, Japan) were bred at 23˚C and fed with sterilized food and water during the experiments. All animal experimental protocols were reviewed and approved by the ethics committee (Animal Care and Use Committee) of Okayama University under the project identification code IDs OKU-2016078 (Date of approval: 1 April 2016).

- **Preparation of anti-hCD44 MAb**

To produce anti-hCD44 MAb, hybridoma Hermes-3 cells (HB-9480, ATCC, VA) cells were cultured using a bioreactor, miniPERM (SARSTEDT, Nümbrecht, Germany). Twenty million of the cells were suspended in 50 mL of PFHM-II (Gibco, NY, USA) medium and were transferred into production module. The production module was connected to nutrient module containing 350 mL of PFHM-II. The bioreactor was rotated for 10 days at 37˚C in 5% CO2. The medium in production module was then collected and centrifuged at 150 xg for 5 min at 4˚C to remove the cells. The supernatant was re-centrifuged at 10,000 xg for 5 min at 4˚C. The supernatant was then passed through 0.20 µm filter (Sartorius Stedim Biotech GmBH, Geottingen, Germany) to completely remove cell debris. Anti-hCD44 MAb was then purified as follows. The supernatant was passed through a 0.5 mL of Protein A Sepharose (GE Healthcare, Uppsala, Sweden) equilibrated with PBS. After washing the column with PBS, anti-hCD44 MAb was eluted using 0.1 M sodium-acetic buffer at pH 2.6. Five hundred µL of each fraction was readily neutralized with 10 µL of 2 M sodium phosphate buffer, pH 8.0. The fraction containing anti-hCD44 MAb was detected by western blotting using polyclonal anti mouse IgG HRP (DAKO, Denmark) and the protein concentration was determined using a BCA assay kit (Pierce Biotechnology, Rockford, IL, USA).

- **Expression of CD44 in Ovarian Cancer Cells line**

  - ***Western blotting***

Proteins following the SDS-PAGE were transferred to polyvinylidene difluoride (PVDF) membranes (Merck Millipore, Burlington, MA, USA). To detect CD44 epitope, the blot was probed using anti-hCD44 MAb (2 mg/mL, 1:2000) followed by polyclonal anti-mouse IgG HRP (1:4000) (DAKO, Denmark). Quantitative assessment of relative intensity of the blots were analyzed using ImageJ. The actin

immunoreact to anti-beta actin Rabbit MAb (1:1000, 4970S, Cell Signalling Technology, Inc., Beverly, MA, USA) was used as a normalization control.

- ***RNA Isolation and Reverse Transcriptional Quantitative PCR (rt-qPCR)***

RNAeasy Mini kit (QIAGEN, Hilden, Germany) was used to isolate total RNA from cells and the extracted RNA was treated with DNase I (Promega, Fitchburg, WI, USA). One μg of RNA was reverse transcribed using GoScript™ Reverse Transcription System (Promega, Fitchburg, WI, USA). qPCR assays were done by LightCycler 480 II (Roche Diagnostics GmbH, Mannheim, Germany) using LightCycler 480 SYBR green I Master Mix (Roche Diagnostics GmbH, Mannheim, Germany) according to the manufacturer's instructions. Gene expression level was normalized with Glyceraldehyde-3-phosphate dehydrogenase GAPDH mRNA. The primers used for the rt-qPCR analysis are listed in Table 2 below.

Table S1. List of primers used in the experiments.

No	Names	Forward primer Sequence (5'->3')	Reverse primer Sequence (5'->3')
1	CD44s	TGGGTTCATAGAAGGGCACG	AGGTGGAGCTGAAGCATTGAA
2	GAPDH	CAACGACCACTTTGTCAAGCTC	GGTCTACATGGCAACTGTGAGG

- ***Flow cytometry analysis***

SK-OV-3 cells and OVK18 cells were harvested at logarithmic growth phase, followed by being re-suspended in 100ul PBS, stained with APC labelled mouse anti-human CD44 MAb (BD Science Pharmingen, San Diego, CA, USA) and FITC labelled mouse anti-human CD24 MAb (BD Science Pharmingen, San Diego, CA, USA), and analyzed by BD AccuriTM C6 plus flow cytometer (Becton & Dickinson,

Franklin Lakes, NJ, USA). Data of each experiment was analyzed using FlowJo software (FlowJo, LLC, Ashland, OR, USA).

- **Preparation of Liposome Encapsulating gPTX**

  - ***Preparation of gPTX-L***

This preparation was conducted with modified of previous method[11]. Liposomes composed of DPPC and Cholesterol (by ratio 3:1) with 5 mol% mPEG–DSPE were prepared by the thin-film hydration method. In brief, DPPC and Chol with 5 mol% mPEG–DSPE were dissolved in an organic solvent of chloroform/methanol (9:1 v/v) in an egg flask. The flask was connected to a rotary evaporator (Eyela, Shanghai, China), which was maintained at 50˚C under aspirator vacuum. The resulting lipid film was left overnight under vacuum to remove remaining organic solvent. The fully dehydrated lipid film was suspended in CEP by vortexing at 60˚C, resulting in the formation of multilamellar vesicles (MLVs).

MLVs were frozen and thawed for five cycles. A single freeze-thaw cycle consisted of freezing at -196˚C liquid nitrogen for 1 min and thawing at 55˚C water bath for 1 min. The liposomes were then extruded 10 times through a single stack of one 100 nm Whatman polycarbonate membranes (GE Healthcare, Carlsbad, CA, USA) using the Mini Extruder (Avanti Polar Lipids, Inc., Alabaster, AL, USA) to form small lamellar vesicles (SLVs). The extruder was kept warm at 55˚C on hot plate prior to extrusion. The outer solvent of the liposomes was replaced CEP with PBS by ultrafiltration with a 100K-membrane filter (Merck Millipore Ltd., Billerica, USA) at 5000 xg for 20 min for five times. Then, gPTX (1 mg/mL) in 40% EG was added into the solution of liposome encapsulating CEP (CEP-L) at 60˚C. gPTX-L was then concentrated to the volume before added drug by ultrafiltration. This encapsulation process was conducted three times. Finally, residual gPTX was removed by washing the liposomes with PBS followed by ultrafiltration at 5000 xg for 20 min for five times.

- ***Preparation of gPTX-IL***

CEP-L composed of DPPC and Chol (by ratio 3:1) with 4 mol% mPEG–DSPE was incubated with 0.5 mol% Mal–PEG–DSPE at 50˚C for 10 min to introduce maleimide functional groups into liposome to conjugate antibodies. Then, gPTX was encapsulated using the solubility gradient method described above. To immobilize antibody on the surface of the liposomes, SH groups were introduced into anti-hCD44 MAb by treatment with 2- iminothiolane (Sigma–Aldrich, St. Louis, MO, USA) at a molar ratio of 1:50 in 25 mM HEPES, pH 8.0 containing 140 mM NaCl. The mixture was subsequently incubated for 1 h at room temperature in the dark. After removing unreacted 2-iminothiolane gel filtration with a G25 PD-10 column (GE Healthcare, Uppsala, Sweden), the modified anti-hCD44 MAb was incubated with liposomes containing Mal–PEG–DSPE overnight at 4˚C. To block free maleimide groups, liposomes were then incubated with L-Cystein (0.5 mM final concentration) for 15 minutes at 25 ˚C. Residual of L-Cystein was removed by ultrafiltration with a 100K-membrane filter 5000 xg for 20 min for five times and followed by removing free anti-hCD44 MAb by ultrafiltration with a 300K membrane filter (Sartorius Stedim Biotech GmbH, Gottingen, Germany) at 6000 xg for 20 min at 4˚C.

- **Evaluation of Cellular Uptake**

- ***Preparation of Fluorescent Liposome***

Lipid composition and hydration step as same as gPTX-L preparation for fluorescent liposome. gPTX replaced by solution of 5 mmol 6-Carboxyfluorescein (FAM) (Molecular Probes Inc, Eugene, OR, USA) in PBS. The fully dehydrated lipid film was suspended by the FAM solution in PBS to produce FAM- liposome (FAM-L) by the direct encapsulation. To prepare FAM Immunoliposome (FAM-IL), Anti-CD44 MAb was conjugated by the same procedure used for conjugation in gPTX-IL.

- ***Confocal Microscopic Observation***

SK-OV-3 cells and OVK18 cells were seeded on gelatin-coated 18 mm coverslip (Iwaki, Japan) in 12-well plates. The cells were incubated with 1μM FAM-L and FAM-IL in serum free medium for 2 hour at 37˚C in an atmosphere of 5% CO_2. The cells were washed three times with cold PBS and fixed with 4% paraformaldehyde in PBS. The coverslips were placed on the slide that already mounted with mounting-solution reagent containing DAPI (Vector Lab, Burlingame, CA, USA) then visualized under a confocal microscope (Fluoview FV-1000, Olympus, Tokyo, Japan).

- ***Flow Cytometry Observation***

SK-OV-3 cells and OVK18 cells were seeded $1x10^5$ cells/well at the 12-well plates. After incubation at 37˚C in 5%CO_2 for 24 h, 1μM FAM-L and FAM-IL were applied for 1 hour and 3 hours in serum free medium. Cells were trypsinized, washed by PBS three times, followed by being re-suspended in 300μl PBS and analyzed by BD Accuri C6 plus flow cytometer (Becton & Dickinson, Franklin Lakes, NJ, USA). Data of each experiment was analyzed using FlowJo®software (FlowJo, LLC, Ashland, OR, USA).

- **Characterization of Liposome**

- ***Size Distribution of Particle and Zeta Potential***

The size and zeta potential of liposomes were determined by dynamic and electrophoretic light scattering using an ELS-8000 (Photal Otsuka Electronics, Osaka, Japan).

- ***Evaluation of Encapsulation efficiency (EE) and loading efficiency (LE)***

EE was calculated as the ratio of the amount of gPTX encapsulated into liposomes to the initial amount of the drug. LE was calculated as the molar ratio of the drug encapsulated into liposomes to the total lipid and chol. The amount of encapsulated

drug was evaluated by C18 reverse-phase HPLC (Hitachi Elite LaChrom L-2400, Tokyo, Japan) under an isocratic condition of 60% (v/v) methanol at a flow rate of 1 mL/min. Ten µL of each sample were injected and the drug was detected at 227 nm.

- ***Transmission electron microscopy (TEM)***

A 400-mesh copper grid coated with formvar/carbon films was hydrophilically treated. Liposome suspension (5 to 10 µL) was placed on Parafilm, and the grid was floated on that suspension and left for 15 min. The sample was negatively stained with 2% uranyl acetate solution for 2 min. liposome on the grid were visualized with 20,000 times magnification with an H-7650 transmission electron microscope (Hitachi, Tokyo, Japan) at Central Research Laboratory, Okayama University Medical School.

- **Cytotoxicity Assay**

- ***Drug Sensitivity Evaluation***

Prior to the evaluation, we tried to optimize the conditions to observe the drug sensitivity. For SK-OV-3 cells, we compared two conditions after exposure of drugs for 72 h. One is to add MTT directly after the exposure and the other is to add MTT following the incubation for 48 h after the drug exposure (Figure S1). Evaluation of IC_{50} was not possible when MTT was directly added after 72 h of drug exposure. Extended incubation for 48 h without drug just after the treatment allowed to evaluate the IC_{50}. For OVK18 cells the evaluation was possible to evaluate the IC_{50} when MTT was added just after the treatment with drug for 72 h. The extended incubation of further 48 h was not adequate for the evaluation of cytotoxic effect on OVK18 cells because the survived cells reached to overgrowth, which affected on the cell growth. Drug sensitivity was checked by MTT assay after 72 h (OVK18) and 120 h (SK-OV-3). Cells were seeded in a 96-well plate at 5000 cells/well. After incubation at 37˚C in 5%CO_2 for 24 h, different concentrations PTX and gPTX were added to each well. For OVK18, after incubation for 72 h, 4.25 mg/ mL MTT solution was added at a final

concentration of 0.5 mg/mL in each well and the plate was incubated for 4 h. The initially seeded cell number (5000 cells/well) and the drug exposure time (72 h) were fixed in both SK-OV-3 cells and OVK18 cells therefore, the extended of incubation time should not induce any biases. For SK-OV-3 cells, after incubation for 72 h, medium with drug were replaced with fresh medium without drug, and incubation were continued until 48 h, 4.25 mg/mL MTT solution was added at a final concentration of 0.5 mg/mL in each well and the plate was incubated for 4 h. Formed formazan crystals were dissolved with 10% (w/v) SDS in 0.02 N HCl and incubated overnight. Finally, the absorbance of each well was measured at 570 nm using an MTP-800 Lab microplate reader (Corona Electric, Ibaraki, Japan). The experiment was performed in triplicate. IC_{50}s were estimated from the survival curve.

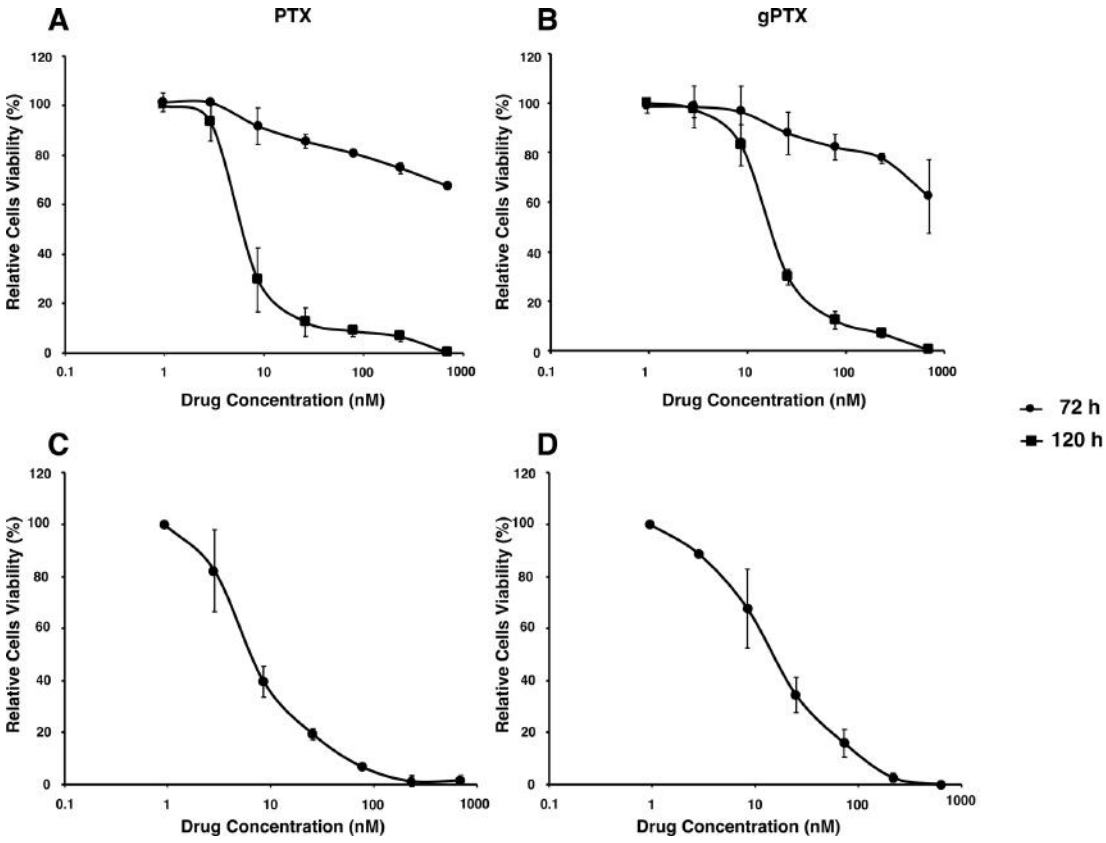

Figure S1. Drug sensitivity evaluation of SK-OV-3 cells (A, B) and OVK18 cells (C,D) after 72 hours drug exposure (closed circle is MTT reagent directly added after

drug treatment, closed square is MTT added after 48 hours drug replaced by fresh medium). (A, C) Cells were treated with PTX. (B, D) Cells were treated with gPTX.

- **Evaluation of cytotoxic effects of liposome formulation by 24h and 72h treatment.**

In vitro cytotoxicity was evaluated by the MTT assay after 72 h (OVK18) and 120 h (SK-OV-3) of cells were seeded in a 96-well plate at 5000 cells/well. After incubation at 37˚C in 5%CO_2 for 24 h, different concentrations gPTX were added to each well. After incubation of drug for 24 h and 72 h, MTT assay was performed as described above.

- **Evaluation of Antitumor Effects of Drugs *In Vivo***

The xenograft of SK-OV-3 cells in mice was prepared by a subcutaneous injection of 7.5 × 10^6 cells/mouse. Tumor volume was measured by a Vernier caliper and calculated as [length × $(width)^2$]/2. Anti-tumor effect of each formulation was evaluated when the tumor volume reached 50–200 mm^3. Mice were randomly assigned to five groups (n = 4); group 1 for PBS, group 2 for CEP, group 3 for CEP-IL, group 4 for naked gPTX, group 5 for gPTX-L and group gPTX-IL. 50 mg of gPTX-equivalent per kg body weight was injected six times via tail vein at the intervals of 4 days. Tumor volumes and body weights were measured at 3 or 4-day intervals. Paraffin embedded liver, kidney, and spleen sections (5-µm thick) were stained with Hematoxylin (Sigma Aldrich,USA;0.5%) and Eosin Y (Sigma Aldrich, USA) (HE) for histological analysis then visualized under FSX100 Inverted Microscope (Olympus, Tokyo, Japan).

- **Statistical Analysis**

All the experiments were repeated at least three-time. Data were depicted as means ± standard deviation. The statistical significance in mean values between two

groups was determined by 2-tailed student's t-test. The statistical significance between the mean values of more than two groups was determined using one-way analysis of variance (ANOVA) and Dunnett's multiple comparisons test. $P<0.05$ was considered statistically significant.

References

1. Siegel, R.L.; Miller, K.D.; Jemal, A. Cancer statistics, 2018. *CA. Cancer J. Clin.* **2018**, *68*, 7–30, doi:10.3322/caac.21442.

2. Torre, L.A.; Bray, F.; Siegel, R.L.; Ferlay, J.; Lortet-Tieulent, J.; Jemal, A. Global cancer statistics, 2012. *CA. Cancer J. Clin.* **2015**, *65*, 87–108, doi:10.3322/caac.21262.

3. Raja, F.A.; Chopra, N.; Ledermann, J.A. Optimal first-line treatment in ovarian cancer. *Ann. Oncol.* **2012**, *23*, x118–x127, doi:10.1093/annonc/mds315.

4. Kampan, N.C.; Madondo, M.T.; McNally, O.M.; Quinn, M.; Plebanski, M. Paclitaxel and Its Evolving Role in the Management of Ovarian Cancer. *Biomed Res. Int.* **2015**, *2015*, 413076, doi:10.1155/2015/413076.

5. Kumar, S.; Mahdi, H.; Bryant, C.; Shah, J.P.; Garg, G.; Munkarah, A. Clinical trials and progress with paclitaxel in ovarian cancer. *Int. J. Womens. Health* **2010**, *2*, 411–27, doi:10.2147/IJWH.S7012.

6. Wu, Y.-J.J.; Neuwelt, A.J.; Muldoon, L.L.; Neuwelt, E.A. Acetaminophen enhances cisplatin- and paclitaxel-mediated cytotoxicity to SKOV3 human ovarian carcinoma. *Anticancer Res.* **2013**, *33*, 2391–400.

7. Gaudy, J.H.; Sicard, J.F.; Lhoste, F.; Boitier, J.F. The effects of cremophor EL in the anaesthetized dog. *Can. J. Anaesth.* **1987**, *34*, 122–129, doi:10.1007/BF03015328.

8. Picard, M.; Pur, L.; Caiado, J.; Giavina-bianchi, P. Risk stratification and skin testing to guide re-exposure in taxane-induced hypersensitivity reactions. *J. Allergy Clin. Immunol.* **2015**, *137*, 1154–1164, doi:10.1016/j.jaci.2015.10.039.

9. Weiss, B.R.B.; Donehower, R.C.; Wiernik, P.H.; Ohnuma, T.; Gralla, R.J.;

Trump, D.L.; Baker, J.R.; Echo, D.A. Van; Hoff, D.D. Von; Leyland-jones, B. Hypersensitivity Reactions From Taxol. **2017**, *8*, 1263–1268.

10. Allen, T.M.; Cullis, P.R. Liposomal drug delivery systems: from concept to clinical applications. *Adv. Drug Deliv. Rev.* **2013**, *65*, 36–48, doi:10.1016/j.addr.2012.09.037.

11. Shigehiro, T.; Kasai, T.; Murakami, M.; Sekhar, S.C.; Tominaga, Y.; Okada, M.; Kudoh, T.; Mizutani, A.; Murakami, H.; Salomon, D.S.; et al. Efficient drug delivery of paclitaxel glycoside: A novel solubility gradient encapsulation into liposomes coupled with immunoliposomes preparation. *PLoS One* **2014**, *9*, doi:10.1371/journal.pone.0107976.

12. Mandai, T.; Okumoto, H.; Oshitari, T.; Nakanishi, K.; Mikuni, K.; Hara, K. ji; Hara, K. zo; Iwatani, W.; Amano, T.; Nakamura, K.; et al. Synthesis and biological evaluation of water soluble taxoids bearing sugar moieties. *Heterocycles* **2001**, *54*, 561–566.

13. Noble, G.T.; Stefanick, J.F.; Ashley, J.D.; Kiziltepe, T.; Bilgicer, B. Ligand-targeted liposome design: challenges and fundamental considerations. *Trends Biotechnol.* **2014**, *32*, 32–45, doi:10.1016/j.tibtech.2013.09.007.

14. Mattheolabakis, G.; Rigas, B.; Constantinides, P.P. Nanodelivery strategies in cancer chemotherapy: Biological rationale and pharmaceutical perspectives. *Nanomedicine* 2012, *7*, 1577–1590.

15. Mattheolabakis, G.; Milane, L.; Singh, A.; Amiji, M.M. Hyaluronic acid targeting of CD44 for cancer therapy: From receptor biology to nanomedicine. *J. Drug Target.* **2015**, *23*, 605–618, doi:10.3109/1061186X.2015.1052072.

16. Sacks, J.D.; Barbolina, M. V Expression and Function of CD44 in Epithelial

Ovarian Carcinoma. *Biomolecules* **2015**, *5*, 3051–66, doi:10.3390/biom5043051.

17. sugii, Y.; kasai, T.; ikeda, masashi; Vaidyanath, arun; kumon, kazuki; mizutani, akifumi; seno, akimasa; Tokutaka, H.; kudoh, T.; seno, masaharu A Unique Procedure to Identify Cell Surface Markers Through a Spherical Self-Organizing Map Applied to DNA Microarray Analysis. *Biomark. Cancer* **2016**, *8*, 17–23, doi:10.4137/BiC.s33542.

18. Mahmud, H.; Kasai, T.; Khayrani, A.C.; Asakura, M.; Oo, A.K.K.; Du, J.; Vaidyanath, A.; El-Ghlban, S.; Mizutani, A.; Seno, A.; et al. Targeting glioblastoma cells expressing CD44 with liposomes encapsulating doxorubicin and displaying chlorotoxin-IgG Fc fusion protein. *Int. J. Mol. Sci.* **2018**, *19*, doi:10.3390/ijms19030659.

19. Orian-Rousseau, V. CD44, a therapeutic target for metastasising tumours. *Eur. J. Cancer* **2010**, *46*, 1271–1277, doi:10.1016/j.ejca.2010.02.024.

20. Zöller, M. CD44 : can a cancer-initiating cell profit from an abundantly expressed molecule ? *Nat. Publ. Gr.* **2011**, *11*, 254–267, doi:10.1038/nrc3023.

21. Shtivelman, E.; Bishop, J.M. Expression of CD44 Is Repressed in Neuroblastoma Cells. *Mol. Cell. Biol.* **1991**, *11*, 5446–5453, doi:10.1128/MCB.11.11.5446.Updated.

22. Bourguignon, L.Y.W.; Peyrollier, K.; Xia, W.; Gilad, E. Hyaluronan-CD44 interaction activates stem cell marker Nanog, Stat-3-mediated MDR1 gene expression, and ankyrin-regulated multidrug efflux in breast and ovarian tumor cells. *J. Biol. Chem.* **2008**, *283*, 17635–17651, doi:10.1074/jbc.M800109200.

23. Oo, A.K.K.; Calle, A.S.; Nair, N.; Mahmud, H.; Vaidyanath, A.; Yamauchi, J.;

Khayrani, A.C.; Du, J.; Alam, M.J.; Seno, A.; et al. Up-Regulation of PI 3-Kinases and the Activation of PI3K-Akt Signaling Pathway in Cancer Stem-Like Cells Through DNA Hypomethylation Mediated by the Cancer Microenvironment. *Transl. Oncol.* **2018**, *11*, 653–663, doi:10.1016/j.tranon.2018.03.001.

24. Ween, M.P.; Oehler, M.K.; Ricciardelli, C. Role of Versican , Hyaluronan and CD44 in Ovarian Cancer Metastasis. **2011**, 1009–1029, doi:10.3390/ijms12021009.

25. Kirpotin, D.; Park, J.W.; Hong, K.; Zalipsky, S.; Li, W.-L.; Carter, P.; Benz, C.C.; Papahadjopoulos, D. Sterically Stabilized Anti-HER2 Immunoliposomes: Design and Targeting to Human Breast Cancer Cells *in Vitro* †. *Biochemistry* **1997**, *36*, 66–75, doi:10.1021/bi962148u.

26. Shigehiro, T.; Masuda, J.; Saito, S.; Khayrani, A.C.; Jinno, K.; Seno, A.; Vaidyanath, A.; Mizutani, A.; Kasai, T.; Murakami, H.; et al. Practical liposomal formulation for taxanes with polyethoxylated castor oil and ethanol with complete encapsulation efficiency and high loading efficiency. *Nanomaterials* **2017**, *7*, doi:10.3390/nano7100290.

27. Loomis, K.; Smith, B.; Feng, Y.; Garg, H.; Yavlovich, A.; Campbell-Massa, R.; Dimitrov, D.S.; Blumenthal, R.; Xiao, X.; Puri, A. Specific targeting to B cells by lipid-based nanoparticles conjugated with a novel CD22-ScFv. *Exp. Mol. Pathol.* **2010**, *88*, 238–249, doi:10.1016/j.yexmp.2010.01.006.

28. Lozano, N.; Al-ahmady, Z.S.; Beziere, N.S.; Ntziachristos, V.; Kostarelos, K. Monoclonal antibody-targeted PEGylated liposome-ICG encapsulating doxorubicin as a potential theranostic agent. *Int. J. Pharm.* **2015**, *482*, 2–10, doi:10.1016/j.ijpharm.2014.10.045.

29. Steffensen, K.D.; Alvero, A.B.; Yang, Y.; Waldstrøm, M.; Hui, P.; Holmberg, J.C.; Silasi, D.A.; Jakobsen, A.; Rutherford, T.; Mor, G. Prevalence of epithelial ovarian cancer stem cells correlates with recurrence in early-stage ovarian cancer. *J. Oncol.* **2011**, *2011*, doi:10.1155/2011/620523.

30. Shi, M.F.; Jiao, J.; Lu, W.G.; Ye, F.; Ma, D.; Dong, Q.G.; Xie, X. Identification of cancer stem cell-like cells from human epithelial ovarian carcinoma cell line. *Cell. Mol. Life Sci.* **2010**, *67*, 3915–3925, doi:10.1007/s00018-010-0420-9.

31. Meng, E.; Long, B.; Sullivan, P.; McClellan, S.; Finan, M.A.; Reed, E.; Shevde, L.; Rocconi, R.P. CD44+/CD24- ovarian cancer cells demonstrate cancer stem cell properties and correlate to survival. *Clin. Exp. Metastasis* **2012**, *29*, 939–948, doi:10.1007/s10585-012-9482-4.

32. Wei, X.; Dombkowski, D.; Meirelles, K.; Pieretti-Vanmarcke, R.; Szotek, P.P.; Chang, H.L.; Preffer, F.I.; Mueller, P.R.; Teixeira, J.; MacLaughlin, D.T.; et al. Mullerian inhibiting substance preferentially inhibits stem/progenitors in human ovarian cancer cell lines compared with chemotherapeutics. *Proc. Natl. Acad. Sci.* **2010**, *107*, 18874–18879, doi:10.1073/pnas.1012667107.

33. Drummond, D.C.; Meyer, O.; Hong, K.; Kirpotin, D.B.; Papahadjopoulos, D. Optimizing liposomes for delivery of chemotherapeutic agents to solid tumors. *Pharmacol. Rev.* **1999**, *51*, 691–743, doi:VL - 51.

34. Yang, X.; lyer, A.K.; Singh, A.; Choy, E.; Hornicek, F.J.; Amiji, M.M.; Duan, Z. MDR1 siRNA loaded hyaluronic acid-based CD44 targeted nanoparticle systems circumvent paclitaxel resistance in ovarian cancer. *Sci. Rep.* **2015**, *5*, 8509, doi:10.1038/srep08509.

35. Arabi, L.; Badiee, A.; Mosaffa, F.; Jaafari, M.R. Targeting CD44 expressing cancer cells with anti-CD44 monoclonal antibody improves cellular uptake and

antitumor efficacy of liposomal doxorubicin. *J. Control. Release* **2015**, *220*, 275–86, doi:10.1016/j.jconrel.2015.10.044.

36. Howes, M.T.; Kirkham, M.; Riches, J.; Cortese, K.; Walser, P.J.; Simpson, F.; Hill, M.M.; Jones, A.; Lundmark, R.; Lindsay, M.R.; et al. Clathrin-independent carriers form a high capacity endocytic sorting system at the leading edge of migrating cells. *J. Cell Biol.* **2010**, *190*, 675–691, doi:10.1083/jcb.201002119.

37. Qhattal, H.S.S.; Liu, X. Characterization of CD44-mediated cancer cell uptake and intracellular distribution of hyaluronan-grafted liposomes. *Mol. Pharm.* **2011**, *8*, 1233–1246, doi:10.1021/mp2000428.

38. Chaudhary, N.; Gomez, G.A.; Howes, M.T.; Lo, H.P.; McMahon, K.A.; Rae, J.A.; Schieber, N.L.; Hill, M.M.; Gaus, K.; Yap, A.S.; et al. Endocytic Crosstalk: Cavins, Caveolins, and Caveolae Regulate Clathrin-Independent Endocytosis. *PLoS Biol.* **2014**, *12*, doi:10.1371/journal.pbio.1001832.

39. Kirpotin, D.B.; Drummond, D.C.; Shao, Y.; Shalaby, M.R.; Hong, K.; Nielsen, U.B.; Marks, J.D.; Benz, C.C.; Park, J.W. Antibody targeting of long-circulating lipidic nanoparticles does not increase tumor localization but does increase internalization in animal models. *Cancer Res.* **2006**, *66*, 6732–6740, doi:10.1158/0008-5472.CAN-05-4199.

40. Talelli, M.; Oliveira, S.; Rijcken, C.J.F.; Pieters, E.H.E.; Etrych, T.; Ulbrich, K.; van Nostrum, R.C.F.; Storm, G.; Hennink, W.E.; Lammers, T. Intrinsically active nanobody-modified polymeric micelles for tumor-targeted combination therapy. *Biomaterials* **2013**, *34*, 1255–1260, doi:10.1016/j.biomaterials.2012.09.064.

ACKNOWLEDGEMENT

In the name of Allah, The Most Compassionate and The Most Benevolence who bestowed me the enlighten, the truth, the knowledge and with regards to Prophet Muhammad S.A.W for the guidance to the straight path. I thank to Allah for giving me the strength in completing this thesis. May Allah bless me with the ability to continue the good deeds to the community in this field.

Firstly, I would like to express my sincere gratitude and great appreciation to Prof. Masaharu Seno for opening his laboratory door to give me trust and let me to be one of his student. His fatherly advice, guidance, encouragement and personality had inspired me to perform my work ability. He has nurtured me and weaned me to this peak of accomplishment. He genuinely deserves much of my gratefulness for his useful suggestion and contributions in whole of my study journey.

I would like to express my sense of gratitude to Associate Prof: Dr. Nobuhiro Okada and Associate Prof: Dr. Akimasa Seno for their helpful support and guidance. I am thankful for their valuable suggestion and discussion during the entire course of study.

I would like also to express the deepest appreciation to Dr. Tomonari Kasai, for his guidance throughout my research. He taught me how to conduct the research project and how to solve the difficulties. Without his guidance and persistent help, this achievement would not have been possible.

I additional extend my great thank to Dr. Hiroshi Murakami, Dr. Akifumi Mizutani, Dr Arun Vaidnayath, and Dr. Junko Matsuda their kindly help, motivation and valuable idea throughout my study.

I would like to extend my special thanks to Mrs Furuse Kaoru, Mrs. Nobue, and Mrs. Mami Asakura, for their kindness, their assistance also technical support throughout my study.

To Professor Takashi Ohtsuki and Professor Hiroshi Tokumitsu, they genuinely deserve much of my gratefulness for their useful comments and kindly reviewing my thesis.

Special thank should go to Hafizah Mahmud, Aung Ko Ko Oo, Juan Du, Md Jahangir Alam, Said M. Afify, Maram H. Zahra, Miharu Oze, Yuki Mimura, Anna Sanchez Calle, Neha Nair, Tsukasa Shigehiro, and Marta Prieto Villa for their guidance, help, encouragement and supports. My acknowledgement also goes to all the students from the Nano-biotechnology laboratory for their valuable suggestion and their friendliness giving me a wonderful memory of my doctoral course. Without them, this thesis would not have been the same as presented here.

I would like to convey my deepest thank to my families in Indonesia, especially my mother (Sumiyah) for her constant prayer, love and care for my success. Special appreciation to my husband, Heri Setiawan and my beloved son, Abdurrahman Haruki Setiawan, both of them have persistently given me strength, motivation, encouragements when needed, and constant prayer throughout my study. I would never have made this far without their support and love.

I gratefully acknowledge the funding received towards my PhD from SGU (Super Global University) scholarship MEXT (Ministry of Education, Culture, Sports, Science and Technology) Japan.

LIST OF PUBLICATION

(1) Targeting Ovarian Cancer Cells Overexpressing CD44 with Immunoliposomes Encapsulating Glycosylated Paclitaxel.

Apriliana Cahya Khayrani, Hafizah Mahmud, Aung Ko Ko Oo, Maram H. Zahra, Miharu Oze, Juan Du, Md Jahangir Alam, Said M Afify, Hagar A. Abu Quora, Tsukasa Shigehiro, Anna Sanchez Calle, Nobuhiro Okada, Akimasa Seno, Koki Fujita, Hiroki Hamada, Yuhki Seno, Tadakatsu Mandai and Masaharu Seno

International Journal of Molecular Sciences, Vol 20, Issue 5, Pages 1042 (2019)

(2) Use of DNA-generated gold nanoparticles to radiosensitize and eradicate radioresistant glioma stem cell.

Tatsuki Kunoh, Tsutomu Shimura, Tomonari Kasai, Syuji Matsumoto, Hafizah Mahmud, **Apriliana Cahya Khayrani**, Masaharu Seno, Hitoshi Kunoh and Jun Takada.

Nanotechnology, Vol 30, pages 1-11 (2018)

(3) Exogenous Cripto-1 Suppresses Self-Renewal of Cancer Stem Cell Model

Md Jahangir Alam, Ryota Takahashi, Said M. Afify, Aung Ko Ko Oo, Kazuki Kumon, Hend M. Nawara, **Apriliana Cahya Khayrani**, Juan Du, Maram H. Zahra, Akimasa Seno, David S. Salomon and Masaharu Seno.

International Journal of Molecular Sciences, Volume 19, Issue 11, Pages 3345, (2018).

(4) Up-Regulation of PI 3-Kinases and the Activation of PI3K-Akt Signaling Pathway in Cancer Stem-Like Cells Through DNA Hypomethylation Mediated by the Cancer Microenvironment

Aung KoKo Oo, Anna Sanchez Calle, Neha Nair, Hafizah Mahmud, Arun Vaidyanath, Junya Yamauchi, **Apriliana Cahya Khayrani**, Juan Du, Md Jahangir Alam, Akimasa Seno, Akifumi Mizutani, Hiroshi Murakami, Yoshiaki Iwasaki, Ling Chen, Tomonari Kasai and Masaharu Seno

Translational Oncology, Vol 11, Issue 3, (2018)

(5) Targeting Glioblastoma Cells Expressing CD44 with Liposomes Encapsulating Doxorubicin and Displaying Chlorotoxin-IgG Fc Fusion Protein

Hafizah Mahmud, Tomonari Kasai, **Apriliana Cahya Khayrani**, Mami Asakura, Aung Ko Ko Oo, Juan Du, Arun Vaidyanath, Samah El-Ghlban, Akifumi Mizutani, Akimasa Seno, Hiroshi Murakami, Junko Masuda and Masaharu Seno.

International Journal of Molecular Sciences, Volume 19, Issue 3, (2018)

(6) Practical Liposomal Formulation for Taxanes with Polyethoxylated Castor Oil and Ethanol with Complete Encapsulation Efficiency and High Loading Efficiency.

Tsukasa Shigehiro, Junko Masuda, Shoki Saito, **Apriliana C. Khayrani**, Kazumasa Jinno, Akimasa Seno, Arun Vaidyanath, Akifumi Mizutani, Tomonari Kasai, Hiroshi Murakami, Ayano Satoh, Tetsuya Ito, Hiroki Hamada, Yuhki Seno, Tadakatsu Mandai and Masaharu Seno.

Nanomaterials, Volume 7, Issue 10, (2017)

(7) Hyaluronic Acid Mediated Enrichment of CD44 Expressing Glioblastoma Stem Cells in U251MG Xenograft Mouse Model

Arun Vaidyanath, Hafizah Binti Mahmud, **Apriliana Cahya Khayrani**, AungKoKo Oo, Akimasa Seno, Mami Asakura, Tomonari Kasai and Masaharu Seno

Journal of Stem Cell Research &Therapy, Vol.7, No.384 (2017)

(8) A new PDAC mouse model originated from iPSCs-converted pancreatic cancer stem cells (CSCcm)

Anna Sanchez Calle, Neha Nair, Aung KoKo Oo, Marta Prieto-Vila, Megumi Koga, **Apriliana Cahya Khayrani**, Maram Hussein, Laura Hurley, Arun Vaidyanath, Akimasa Seno, Yoshiaki Iwasaki, Malu Calle, Tomonari Kasai, Masaharu Seno.

American journal of cancer research, Vol: 6 (12) pp: 2799-2815 (2016)

(9) Functional Characterization of Group II Chaperonin and Prefoldin From *Hyperthermophilic Thermoccus sp.* KS-1 In Inorganic Co-Solvent.

Muhamad Sahlan, **Apriliana Cahya Khayrani,** Neng Risma Liasari.

International Journal of Pharma and Bio Sciences, Vol 2, Issue 2 (2011)

ORAL AND POSTER PRESENTATION

(1) Evaluation of Glycosylated Paclitaxel Encapsulated into Liposomes Conjugated with Anti-CD44 Antibody to Target Ovarian Cancer **(Poster Presentation)**

Apriliana Cahya Khayrani, Hafizah Mahmud, Aung Ko Ko Oo, Tomonari Kasai, Maram Hussein Zaky Zahra, Tsukasa Shigehiro, Juan Du, Koji Hara, Hiroki Hamada, Yuhki Seno, Tadakatsu Mandai, Said M Afify, Masaharu Seno

MBSJ The 41st Annual Meeting of the Molecular Biology Society of Japan, The Molecular Biology Society of Japan, 2P-0646 (Yokohama, 2018-11-28)

(2) Development of Paclitaxel Glycoside Liposomes Conjugated with Anti-CD44 Antibody Targeting Ovarian Cancer Cells **(Oral Presentation)**

Apriliana Cahya Khayrani, Hafizah Mahmud, Tomonari Kasai, Aung Ko Ko Oo, Juan Du, Md Jahangir Alam, Koji Hara, Hiroki Hamada, Yuhki Seno, Said M Afify, Tadakatsu Mandai, Masaharu Seno

The 77th Annual Meeting of the Japanese Cancer Association, Japanese Cancer Association, E-3052 (Osaka, 2018-09-29)

(3) Delivery of Liposomal Paclitaxel Glycoside to Glioblastoma Cells Targeting CD44 **(Poster Presentation)**

Apriliana Cahya Khayrani, Tomonari Kasai, Hafizah Mahmud, Tsukasa Shigehiro, Arun Vaidyanath, Aung Ko Ko Oo, Koji Hara, Hiroki Yamada, Yuhki Seno, Takadatsu Mandai, Du Juan, Masaharu Seno

Consortium of Biological Sciences 2017, The 40th Annual Meeting of the Molecular Biology Society of Japan, The 90th Annual Meeting of the Japanese Biochemical Society of Japan, The Japanese Biochemical Society/The Molecular Biology Society of Japan, 2P-0810 (Kobe, 2017-12-07)

(4) Targeting of glioblastoma with multivalent of anti-CD44 antibody-paclitaxel glycoside liposomes

Apriliana Cahya Khayrani, Tomonari Kasai, Hafizah Mahmud, Tsukasa Shigehiro, Arun Vaidyanath, Aung Ko Ko Oo, Masaharu Seno. **(Poster Presentation)**

The International Conference and Exhibition on Nanomedicine and Drug Delivery (Osaka, 2017-05-30)